European Journal of Taxonomy 1098: 1–34
https://doi.org/10.5852/ejt.2026.1098.3329

europeanjournaloftaxonomy.eu
ISSN 2118-9773
2026 · Watanabe K. *et al.*

Received: 19 March 2026 • *Accepted: 25 June 2026* • *Published: 23 September 2026*

Topic editor: Tony Robillard • *Section editor: Karen Salazar* • *Desk editor: Pepe Fernández*

Research article

urn:lsid:zoobank.org:pub:FF54CDD8-836C-4488-A184-16848BE9255E

Austrelatus zimmermanni (Gschwendtner, 1934) comb. nov. (Coleoptera: Dytiscidae: Copelatinae) with two new subspecies from Japan, and notes on the species biology and ecology

Kohei WATANABE [1,*], Masaya KATO [2,*], Shouhei UEDA [3] & Helena SHAVERDO [4]

[1] Ishikawa Insect Museum, Hakusan, Ishikawa 920–2113 Japan.
[1] The Kyushu University Museum, Fukuoka 812–8581 Japan.
[2,3] Graduate School of Agriculture, Osaka Metropolitan University, Sakai, Osaka 599–8531 Japan.
[4] Naturhistorisches Museum Wien, Burgring 7, 1010, Vienna, Austria.

[*] Corresponding authors: [1] koutarouhigasi@yahoo.co.jp – [2] kato.m.68n047@gmail.com
[3] Email: sueda@omu.ac.jp
[4] Email: Helena.Shaverdo@nhm.at

Abstract. Museum specimens and the newly collected material of the species known so far as *Copelatus zimmermanni* Gschwendtner, 1934 from Japan were examined, and based on our molecular analysis and morphological study, the species is recognised to belong to the genus *Austrelatus* Shaverdo, Hájek, Hendrich, Surbakti, Panjaitan & Balke, 2023: *Austrelatus zimmermanni* (Gschwendtner, 1934) comb. nov. Although showing almost no differences in the shape of the male genitalia, specimens from the Minamidaitô-jima and Miyako-jima islands have a very distinct external morphology from those of other localities and, therefore, are described here as two new subspecies: *A. zimmermanni daitoensis* Watanabe, Kato & Shaverdo subsp. nov. and *A. zimmermanni miyakoensis* Watanabe, Kato & Shaverdo subsp. nov., which is also supported by the received molecular data. Their important diagnostic characters are compared with those of the nominotypical subspecies and illustrated. In comparison with the Chinese and Korean material, a taxonomic problem of *A. zimmermanni* is postulated and discussed. Data on the species ecology and distribution, including its two subspecies, are provided as well as the newly received data on its biology and phenology.

Keywords. Aquatic insects, new combination, diving beetle, taxonomy, phenology, molecular phylogenetic analysis.

Watanabe K., Kato M., Ueda S. & Shaverdo H. 2026. *Austrelatus zimmermanni* (Gschwendtner, 1934) comb. nov. (Coleoptera: Dytiscidae: Copelatinae) with two new subspecies from Japan, and notes on the species biology and ecology. *European Journal of Taxonomy* 1098: 1–34. https://doi.org/10.5852/ejt.2026.1098.3329

Introduction

With 896 species, Copelatinae Branden, 1884 is the second most species-rich subfamily of Dytiscidae Leach, 1815, representatives of which are mostly distributed in the tropical and sub-tropical zones worldwide (Nilsson & Hájek 2026). It includes nine genera, of which *Copelatus* Erichson, 1832, *Exocelina* Broun, 1886, and *Australatus* Shaverdo, Hájek, Hendrich, Surbakti, Panjaitan & Balke, 2023 comprise most of the species, viz. 451, 216, and 106, respectively. These genera are also the groups to which a majority of the newly discovered species belong (e.g., Shaverdo *et al.* 2012, 2023, 2024; Sheth *et al.* 2018; Ranarilalatiana & Bergsten 2019; Ranarilalatiana *et al.* 2019; Hájek *et al.* 2021, 2024; Jiang *et al.* 2022, 2025, 2026; Shaverdo & Balke 2022; Hájek & Shaverdo 2024) and for which many new species can still be expected. For example, the genus *Australatus*, recently described for 62 Australasian species and replenished with 42 new species from New Guinea (Shaverdo *et al.* 2024) and two new species from the Oriental Region (Hájek & Shaverdo 2024), is estimated to have many more species in Australasia (Shaverdo *et al.* 2026 in prep.).

In Japan, the Copelatinae is represented by two genera: *Australatus* with one species, *A. parallelus* (Zimmermann, 1920), and *Copelatus* with 13 species (Nakajima *et al*. 2020; Watanabe & Yoshitomi 2022). *Copelatus zimmermanni* Gschwendtner, 1934 was originally placed in the *C. nigrolineatus* species group (Guéorguiev 1968). However, after *C. nigrolineatus* Sharp, 1882 was recently transferred to *Australatus* (Shaverdo *et al.* 2023), the group was renamed the *C. zimmermanni* species group, which is characterised by (11–12)+0 elytral striae and includes four species worldwide (Nilsson & Hájek 2026). We discovered that this species is the second representative of the genus *Australatus* in the Japanese dytiscid fauna and is very polymorphic, having two distinct subspecies on the Minamidaitô-jima and Miyako-jima islands, which we describe here in detail. Also, we discuss a problem with the species' taxonomic position and provide data on its biology, ecology, molecular phylogeny, and distribution.

Material and methods

Material studied

The present work is based on material deposited in the following collections:

AAC = Atsushi Aimoto Collection, Yamaguchi, Japan
EUMJ = Ehime University Museum, Matsuyama, Japan
IIM = Ishikawa Insect Museum, Hakusan, Japan
NHMW = Naturhistorisches Museum Wien, Vienna, Austria
NMPC = National Museum of the Czech Republic, Prague, Czech Republic
OMNH = Osaka Museum of Natural History, Osaka, Japan

Detailed information on all studied specimens is provided below. Material of *Australatus z. zimmermanni* from Japan is given in the part about the species distribution in the country and organised by the regions and prefectures, following information on the administrative division of Japan from Wikipedia (2026). A map of the sampling sites (Fig. 6) was generated using QGIS ver. 3.34.11-Prizren (QGIS Development Team 2024).

The label data of the types of the new subspecies are given before their descriptions. The type specimens are provided with corresponding red (holotypes) and light blue (paratypes) printed labels.

Morphological study and photography

The specimens were observed using a stereoscopic microscope (Nikon SMZ-1500, HR Plan Apo, 1×) and measured using a stereoscopic microscope (Leica M205C, Planapo 1.0×) with a Leica DFC420 camera and LAS software ver. 3.3.1. Photographs were taken using Nikon D500 digital cameras equipped

with a Laowa ULTRA MACRO 25 mm f/2.8 2.5–5× (Figs 1A–C, 3A, C–E) and a Nikon AF-S VR Micro NIKKOR 105 mm f/2.8G ED lens (Figs 2, 3B), as well as a stereoscopic microscope (Nikon SMZ-1500, HR Plan Apo, 1×) with a Sony αILCE-QX1 digital camera (Figs 1D–I, 4B–G, I–T) and an optical microscope (Nikon ECLIPSE E400) with an Olympus OM-D E-M5 Mark II digital camera (Fig. 4A, H). Multiple digital photographs were combined by focus stacking using the digital image processing software Zerene Stacker ver. 1.04 (Zerene Systems LLC, USA) (Figs 1, 4). The abbreviations and terms used in this study mostly follow those of Shaverdo *et al*. (2023): DBE = minimum distance between eyes; EL = elytral length; MW = maximum width; PL = pronotal length; PW = pronotal width at the level of the posterior margin; TBL = transverse basal band on elytra length; TL = total length; TL-h = total length minus head length. The orientation of the genitalia follows Miller & Nilsson (2003). Morphological descriptions, including terminology of the medial lobe parts, follow Shaverdo *et al*. (2023, 2024).

Comparisons of TL-h among specimens of *Austrelatus zimmermanni* comb. nov., *A. z. daitoensis* Watanabe, Kato & Shaverdo subsp. nov., and *A. z. miyakoensis* Watanabe, Kato & Shaverdo subsp. nov. were assessed using one-way analysis of variance (ANOVA) followed by the Tukey-Kramer post hoc test. TL-h/MW and TBL/EL ratios for the three subspecies were analysed using the non-parametric Kruskal-Wallis test, and pairwise comparisons were made using the Wilcoxon rank-sum test with continuity correction (*P*-value adjustment by Holm's method). TL-h and TL-h/MW were compared separately for males and females, while TBL/EL was compared collectively for both sexes. All analyses were conducted using R ver. 4.4.1 (R Core Team 2020).

Laboratory rearing and comparison of larval periods of five species of Copelatinae

Eight adults (four pairs) of *Austrelatus z. miyakoensis* subsp. nov. were collected from the type locality. Rearing was conducted following previously described methods (e.g., Watanabe *et al*. 2017; Watanabe & Ohba 2022). Java moss (Hypnaceae) and 3 cm of water were placed in clear plastic cups (13 cm diameter and 6 cm height) to provide shelter and oviposition sites for the adults. The adults were fed an adequate amount of frozen chironomid larvae every 2–3 days. The rearing containers were examined daily for eggs by hand-washing the Java moss in water. The date of egg detection was recorded, and the eggs were transferred to individual clear plastic 'larval cups' (8 cm diameter, 4 cm height, 5 mm water depth).

Living chironomid larvae and tubificid worms (obtained from the Ishikawa Insect Museum) were provided daily as larval prey, as previously described (e.g., Watanabe *et al*. 2017; Watanabe & Ohba 2022). For pupation, plastic 'pupation cups' (same size as larval cups) were prepared with crushed and moistened peat moss (1 cm depth) as a landing soil substrate. In the third instar, when the larvae ceased to consume prey, walked continuously, and had invisible midgut content, individual larvae were carefully placed in their pupation cups. Observations of hatching, molting, transition to the soil, and dates of emergence of adults from the pupal chamber to the soil surface were recorded every 24 h. The rearing room was maintained at 26°C with a 9 h light and 15 h dark (9L : 15D) photoperiod.

To compare larval periods, previously published data for *Austrelatus parallelus* (Watanabe *et al*. 2017), *A. zimmermanni* (Watanabe & Ohba 2022), *Copelatus kammuriensis* Tamu & Tsukamoto, 1955 (Watanabe *et al*. 2024), *C. masculinus* Régimbart, 1899 (Watanabe & Hayashi 2019), and *C. nakamurai* Guéorguiev, 1970 (Watanabe 2022), which were reared under the same conditions as those in this study, were used. The total larval period for the five species, including *A. z. miyakoensis* subsp. nov. obtained in this study was analysed using the non-parametric Kruskal-Wallis test, and pairwise comparisons were made using the Wilcoxon rank-sum test with continuity correction (*P*-value adjustment by Holm's method). All analyses were conducted using R ver. 4.4.1 (R Core Team 2020).

Samples and DNA extraction

Samples of Japanese *Austrelatus zimmermanni* were collected at 11 sites in Honshu (Akita Prefecture: laboratory-reared individual), Kyushu (Fukuoka Prefecture, Nagasaki Prefecture), Tsushima Island, the Nansei Islands (Tanega-shima Island, Nakano-shima Island, Kakeroma-jima Island, Okinawa-jima Island, Kume-jima Island, Minamidaitô-jima Island, Miyako-jima Island). *Austrelatus zimmermanni* is generally known to have a low population density in its habitat (Nakajima *et al*. 2020), and in the present study, we were unable to collect many samples from each locality. Therefore, one to two samples from each locality were used for the molecular phylogenetic analyses. Since the collection of insects is prohibited at Nakano-shima Island and Kume-jima Island by local ordinances, permissions were obtained from Toshima Village (permission number: 2520) and Kumejima-chô (permission number: 969) before conducting the survey. Three additional species of Copelatinae were used in the molecular analyses: *Copelatus kammuriensis* Tamu & Tsukamoto, 1955, and *C. oblitus* Sharp, 1882, collected from Osaka Prefecture and the Nansei Islands (Iriomote-jima Island), and *Austrelatus parallelus* (Zimmermann, 1920), collected from Shiga Prefecture, as well as *Hydrovatus stridulus* Biström, 1997, collected from Shizuoka Prefecture, which was used as an outgroup of Copelatinae. Additionally, sequences of *Copelatus chevrolati* Aubé, 1838, *C. japonicus* Sharp, 1884, *C. neelumae* Vazirani, 1973, *C. teranishii* Kamiya, 1938, and *C. weymarni* Balfour-Browne, 1947 from GenBank (accession numbers HM433233, OL663317, MW580697, LC727323, and LC797044, respectively) were used for a phylogenetic analysis. All samples were preserved in 99% ethanol and used in a molecular phylogenetic analysis. Genomic DNA was extracted from one hind leg using the DNeasy Blood & Tissue Kit (Qiagen, Hilden).

DNA sequencing

For the amplification of the partial mitochondrial DNA (mtDNA) *COI* gene and nuclear DNA (nDNA) *histone 3* gene, we used 17 samples of *Austrelatus zimmermanni*, and one sample each of *Copelatus kammuriensis*, *C. oblitus*, *A. parallelus*, and *Hydrovatus stridulus*. PCRs were conducted using the primers LCO1490 (5′-GGTCAACAAATCATAAAGATATTGG-3′) and HCO2198 (5′-TAAACTTCAGGGTGACCAAAAAATCA-3′) (Folmer *et al*. 1994) for the mtDNA *COI* gene, H3aF (5′-ATGGCTCGTACCAAGCAGAC(AG)CGC-3′) and H3aR (5′-ATATCCTT(AG)GGCAT(AG) AT(AG)GTGAC-3′) (Colgan *et al*. 1998) for the nDNA *histone 3* gene. The compositions of the PCR reaction mixtures for amplifying the mtDNA *COI* gene and nDNA *histone 3* gene were as follows: 1.0 µL of template DNA (<5 ng), 5.0 µL of KOD One® PCR Master Mix (TOYOBO, Japan), 0.3 µL of each primer (10 µM), a final volume of 10 µL. The PCR cycling conditions for mtDNA *COI* gene were as follows: an initial denaturation at 98°C for 5 min, followed by 35 cycles of denaturation at 98°C for 10 sec, annealing at 47°C for 30 sec, and extension at 72°C for 1 min, with a final extension at 72°C for 7 min. The PCR cycling conditions for nDNA *histone 3* gene were as follows: an initial denaturation at 96°C for 3 min, followed by 40 cycles of denaturation at 94°C for 30 sec, annealing at 49°C for 1 min, and extension at 72°C for 1 min, with a final extension at 72°C for 10 min. PCR products were purified using ExoSAP-IT (Applied Biosystems, USA). Purified PCR products were used for cycle sequencing with BigDye™ Terminator ver. 3.1 Cycle Sequencing Kit (Applied Biosystems, USA), and the compositions of the mixtures were as follows: 1.0 µL of purified PCR products, 0.4 µL of BigDye™ Terminator ver. 3.1 Ready Reaction Mix, 1.8 µL of 5X Sequencing Buffer, 0.2 µL of each primer (10 µM), and a final volume of 10 µL. The PCR cycling conditions for cycle sequencing were as follows: an initial denaturation at 96°C for 1 min, followed by 25 cycles of denaturation at 96°C for 10 sec, annealing at 50°C for 5 sec, and extension at 60°C for 4 min. After cycle sequencing, PCR products were sequenced by ABI PRISM 3130 Genetic Analyzer (Applied Biosystems, USA). Sequence data were edited and aligned for each gene separately using MEGA11 (Tamura *et al*. 2021) and ClustalW (Thompson *et al*. 1994).

Phylogenetic analysis based on mitochondrial and nuclear DNA

The maximum likelihood (ML) tree was generated based on the dataset 1 (the mtDNA *COI* gene 599 bp and the nDNA *histone 3* gene 301 bp) and the dataset 2 (the mtDNA *COI* gene 599 bp), using IQ-TREE

ver. 3.1.2 (Wong *et al*. 2026), with ultrafast bootstrap analysis (1000 replicates), excluding samples with identical sequences. The nucleotide substitution models were selected based on the BIC value using ModelFinder (Kalyaanamoorthy *et al*. 2017) within IQ-TREE ver. 3.1.2. For the dataset 1, GTR+F+G4 was selected as the optimal model for the mtDNA *COI* gene, whereas HKY+F+G4 was selected for the nDNA *histone 3* gene. For the dataset 2, TVM+F+G4 was selected. The phylogenetic tree was drawn and edited using FigTree ver. 1.4.4 (Rambaut 2009). Additionally, the median joining haplotype network was estimated based on the mtDNA *COI* gene 599 bp, using PopART ver. 1.7 (Leigh & Bryant 2015), with all *Austrelatus zimmermanni* samples included. The genetic distances (pairwise distances) between haplotypes were calculated using MEGA11.

MIG-seq analysis

MIG-seq is a PCR-based method that identifies genome-wide single-nucleotide polymorphisms (SNPs) from inter-simple sequence repeats (ISSRs) (Suyama & Matsuki 2015). This method is suitable for investigating genetic differentiation or genetic identification among species, hybrids, and populations (Suyama *et al*. 2022). Therefore, this method is considered to be the most suitable for elucidating the genetic structure of *Austrelatus zimmermanni* in Japan.

For MIG-seq analysis, 11 samples of *A. zimmermanni* were used, collected from Honshu (Akita Prefecture: laboratory-reared individual), Kyushu (Fukuoka Prefecture), and the Nansei Islands (Nakano-shima, Kakeroma-jima, Okinawa-jima, Minamidaitô-jima, and Miyako-jima Islands). Samples were selected to cover all haplotypes identified by the median joining haplotype network analysis. The basic experimental methods for MIG-seq were carried out based on Suyama & Matsuki (2015). The 1st PCR for amplifying the ISSRs was conducted using "MIG-seq primer set 1" by Suyama & Matsuki (2015). The compositions of the 1st PCR reaction mixtures were as follows: 2.0 μL of template DNA (<5 ng), 0.1 μL of Multiplex PCR Mix (Takara, Japan), 0.2 μL of each primer (0.2 μM), 10.0 μL of 2X Multiplex PCR buffer, and a final volume of 20 μL. The 1st PCR cycling conditions were as follows: an initial denaturation at 94°C for 1 min, followed by 25 cycles of denaturation at 94°C for 30 sec, annealing at 38°C for 1 min, and extension at 72°C for 1 min, with a final extension at 72°C for 10 min. The 1st PCR products were used for 2nd PCR, for adding the complementary sequences, using "2nd PCR primers" by Suyama & Matsuki (2015). The compositions of the 2nd PCR reaction mixtures were as follows: 2.5 μL of 50 times diluted 1st PCR products, 2.4 μL of 5X PrimeSTAR GXL Buffer (Takara, Japan), 0.96 μL of dNTP mixture, 1.2 μL of 2nd PCR forward primer (2 μM), 1.2 μL of 2nd PCR reverse primer (2 μM), 0.24 μL of PrimeSTAR GXL polymerase, and a final volume of 12 μL. The 2nd PCR cycling conditions were as follows: 12 cycles of denaturation at 98°C for 10 sec, annealing at 54°C for 15 sec, and extension at 68°C for 1 min. After the 2nd PCR, 1 μL of each PCR product was pooled into a single library and purified with AMPure XP beads (Beckman Coulter Life Sciences, USA). Then, size selection (400–800 bp) of the library was conducted using the BluePippin (Sage Science, Beverly, MA, USA), and the size of the library was measured using the Qubit 4 Fluorometer (Thermo Fisher Scientific, USA). After measuring the size, the library diluted to 12 pM was sequenced on an Illumina MiSeq System (Illumina, San Diego, CA, USA) using a MiSeq Reagent Kit ver. 3 (150 cycles, Illumina).

Low-quality reads and primer sequences were eliminated from the raw data using Trimmomatic ver. 0.39 (Bolger *et al*. 2014). At the same time, sequence reads with a final length less than 80 bases were removed. The quality-filtered sequence reads were demultiplexed and filtered using Stacks ver. 2.68 software (Rochette *et al*. 2019). With 'ustacks', the following option settings were used: minimum depth of coverage required to create a stack (m) = 3, maximum distance allowed between stacks (M) = 2. With 'populations', the following option settings were used: minimum minor allele frequency required to process a nucleotide site at a locus (min_maf) = 0.02, maximum observed heterozygosity needed to process a nucleotide site at a locus (max_obs_het) = 0.5, and minimum proportion of individuals required to process a locus across all data (r) = 0.8.

Molecular analysis based on genome-wide SNPs

The MIG-seq dataset identified 166 SNPs from 11 samples of *Austrelatus zimmermanni* (missing rate: 4.22–16.87%). Genetic structure analysis was conducted based on the SNPs data using STRUCTURE ver. 2.3.4. (Pritchard *et al*. 2009), with the number of clusters (*K*) set from 1 to 7. After a burn-in period of 1.0×10^5 iterations, simulations were performed using Markov chain Monte Carlo (MCMC) method for 1.0×10^5 iterations, with ten independent runs for each *K*. To select the optimal *K*, the Δ*K* value for each *K* was calculated using StructureSelector (Li & Liu 2018), and the *K* with the highest Δ*K* value was considered the optimal number of clusters. The phylogenetic tree based on the MIG-seq dataset was estimated using the neighbor-net method (Bryant & Moulton 2004) with SplitsTree ver. 6.6.5. (Huson & Bryant 2024).

Results

Taxonomy

Class Insecta Linnaeus, 1758
Order Coleoptera Linnaeus, 1758
Family Dytiscidae Leach, 1815
Subfamily Copelatinae Branden, 1884
Tribe Copelatini Branden, 1884
Genus *Austrelatus* Shaverdo, Hájek, Hendrich, Surbakti, Panjaitan & Balke, 2023

Austrelatus zimmermanni (Gschwendtner, 1934) comb. nov.
Figs 1–7

Copelatus zimmermanni Gschwendtner in Zimmermann, 1934: 143 (original description).

Copelatus zimmermanni – Satô 1983: 37; 1985: 65; 1998: 9; 2004: 8. — Matsui 1987: 5; 1988: 6; 1989: 20. — Matsui *et al.* 1988: 75. — Lee 1991: 16. — Ôtsuka 1991: 39. — Sakurai 1992: 21. — ESK & KSAE 1994: 133. — Takahashi 1994: 5. — Iwasaki & Kinoda 1995: 106. — Nomura *et al.* 1996: 251. — Cho & Kim 1998: 60. — Tahira & Kitano 2000: 44. — Mori & Kitayama 2002: 116. — Kamite 2003: 12. — Nakajima & Inoue 2004: 14. — Narukawa *et al*. 2006: 99. — Park *et al.* 2008: 76. — Hosoya *et al.* 2009: 7. — Fukagawa 2015: 32. — Fukagawa *et al.* 2016: 22. — Hosoya & Tanahashi 2017: 15. — Morii 2018: 5. — Aimoto 2018: 27. — Lee & Ahn 2018: 46. — Kamite *et al.* 2019: 22. — Chung *et al*. 2020: 182. — Nakamine & Nakamine 2021: 3. — Miyake 2021: 100. — Imasaka *et al.* 2021: 72. — Jiang *et al.* 2022: 275. — Watanabe & Ohba 2022: 1. — Aoyagi *et al*. 2022: 118. — Kato & Watanabe 2025a: 3; 2025b: 154.

Taxonomic recognition

According to our molecular analysis, *Austrelatus zimmermanni* forms a sister group with *A. parallelus* (see below the Phylogenetic analysis based on the mtDNA and the nDNA), which is also supported by the study of its male genitalia. A complex structure of the median lobe of the aedeagus, with the distinct dorsal and ventral sclerites, as well as the paramere of the narrow triangular form, are the main diagnostic characters of the genus *Austrelatus*. They are applicable for the Australasian species and less to the species from Oriental and Palearctic regions, which have much thinner and simpler median lobes. However, *A. zimmermanni* differs from all Oriental and Palearctic representatives by a very sturdy median lobe, of rather complex form, which mostly consists of the modified, but not divided into two apical lobes, dorsal sclerite. The ventral sclerite is small, membranous, but distinctly visible in ventral view, occupying a large, rounded ventral opening, and is divided into two apical lobes. The species has a paramere of the typical narrow triangular form and weakly impressed, irregular elytral striae, which are sometimes fragmented or absent. Therefore, we recognise the species as *Austrelatus.*

General distribution of *Austrelatus zimmermanni* (Gschwendtner, 1934) and its taxonomic problematic

At present, *Austrelatus zimmermanni* is only known from China, Japan, and South Korea (Nilsson & Hájek 2026) (Fig. 6). The species was described as *Copelatus* by Gschwendtner (Gschwendtner in Zimmermann 1934: 143) from Hangzhou, Zhejiang Province of China – "China (Hangchow)" in the original description. The description was based on a single female deposited in the Yenching University, Beijing, China, and destroyed during a fire in 1980 (Jiang *et al.* 2022: 275). Guéorguiev (1968: 11) referred to the original description and placed the species into the *C. nigrolineatus* group (now *C. zimmermanni* species group), whose representatives have 11–12 dorsal striae on the elytron. Recently, the species was again reported from China, Guangdong Province, by Jiang *et al.* (2022: 275) who provided a diagnosis and photos of the female habitus and male genitalia. In our study, we examined part of the material used in this paper, identified as "*Copelatus zimmermanni*": 3 males, 4 females "CHINA, Guangdong prov. 30 km NE Shaoguan, Duanshi vill. Danxia Shan NP (stream; pools) 25°02.7'N, 113°43.8'E, 125 m Jiří Hájek leg., 4–5.v.2011" (NMPC) and 1 male "CHINA, Guangdong prov. Danxia Shan NP, 25.iv.2013 Yang Juan Shan area (pools) 25°02.7'N, 113°43.8'E, 135 m J. Hájek & J. Růžička leg." (NMPC). Korean records were made by Lee (1991: 16), ESK & KSAE (1994: 133), Cho & Kim (1998: 60) and Park *et al.* (2008: 76). The latter provided the median lobe drawings of the species and summarised the species distribution in Korea as from Jeju ("Jejudo") Island. Lee & Ahn (2018: 46) provided detailed description and figures of habitus and median lobe drawing of the species. The most recent report of the species from the Korean Peninsula is by Chung *et al*. (2020). The majority of the *A. zimmermanni* records are known from Japan, where the species occurs from the North to the very South of the country on the different islands and shows a morphological variability. These records are summarised and treated in detail below.

Our study of the Japanese and Chinese (Guangdong) specimens, as well as the photos in Jiang *et al.* (2022: 275–276, figs 27, 69–70), revealed some differences in their morphology. The Guangdong specimens have a slightly broader habitus and a distinctly broader reddish yellow basal band of the elytron, which reaches almost ¼ of the elytral length (Fig. 5A), than the Japanese specimens (Fig. 1A–C). Their elytron usually has 11 dorsal striae, of which the sutural one can be almost completely reduced. The Japanese specimens are characterised by a more reduced elytral striation, usually with 9–10 dorsal striae (Fig. 1A), but rarely observed with 11 dorsal striae in females. Furthermore, there are distinct differences in the shape of the median lobe. The Guangdong specimens have a left lateral side of the dorsal sclerite much more curved (concave subapically), so that in left lateral view, the median lobe has two distinct projections: dorso-medially (present also in Japanese specimens) and latero-subapically (absent in Japanese specimens, which have instead a large, elongate, flat crest) (Figs 4A–G, 5B). Also, the dorso-medial projection is smaller and has a more pointed apex in the Guangdong specimens than in the Japanese ones, where it is broadly rounded. The apex of the median lobe is straighter, and its tip is more prolongate in the Guangdong specimens (Fig. 5B–C); in Japanese specimens, it is slightly curved downwards and often sturdier (Fig. 4). In right lateral view, the lateral margins of the dorsal sclerite are differently curved, especially apically: the left lateral margin has a much weaker subapical notch and is much more thickened before this notch in the Guangdong specimens (Figs 4H–N, 5C).

Based on these observations, we think that the Japanese and Chinese (Guangdong) specimens belong to two different species, one of which is *A. zimmermanni* and the other is new. Unfortunately, it is impossible to define which is which because the original description, based on the single female, does not provide the necessary characters, and colouration is too generally described in it. As for the Korean specimens, the median lobe drawings by Park *et al.* (2008: 74, figs 3a–b) are done in the right lateral view, which might conceal the second protuberance, and in the dorsal view, which seems to be wrongly done. Meanwhile, the median lobe in the left lateral view drawings by Lee & Ahn (2018: 142, pl. 14b) is accurate and of the same shape as the median lobe of the Japanese specimens. Therefore, we consider the Korean and Japanese specimens to belong to *A. zimmermanni* since it is assumed to have a similar

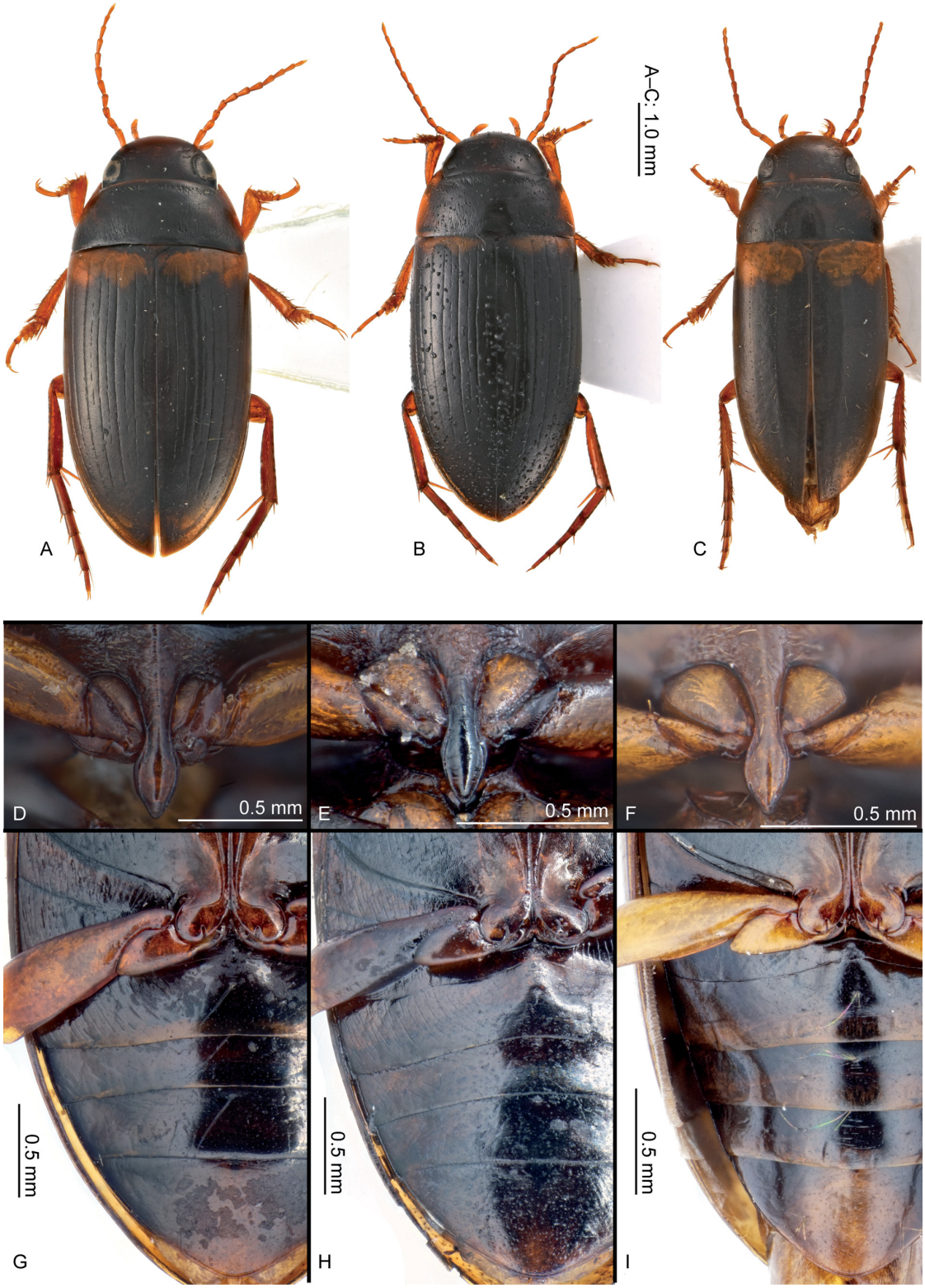

Fig. 1. Males of *Austrelatus zimmermanni* (Gschwendtner, 1934) comb. nov. from Japan. **A, D, G**. *A. z. zimmermanni*, Akita Prefecture (OMNH). **B**. *A. z. daitoensis* Watanabe, Kato & Shaverdo subsp. nov., holotype (EUMJ). **E, H**. *A. z. daitoensis,* paratypes (IIM), Minamidaitô-jima Island. **C, F, I**. *A. z. miyakoensis* Watanabe, Kato & Shaverdo subsp. nov., holotype, Miyako-jima Island (EUMJ). **A–C**. Habitus, dorsal view. **D–F**. Prosternal process. **G–I**. Metacoxal process and abdomen.

Fig. 2. Live specimens of *Austrelatus zimmermanni miyakoensis* Watanabe, Kato & Shaverdo subsp. nov., paratypes (IIM). **A**. Male. **B**. Female. The magnification differs between males and females.

Fig. 3. Photos of the different life stages of *Austrelatus zimmermanni miyakoensis* Watanabe, Kato & Shaverdo subsp. nov. **A**. Egg. **B**. New adult escaping to the soil surface. **C**. Instar I. **D**. Instar II. **E**. Instar III.

distribution to that of some other species of Copelatinae (e.g., *Copelatus japonicus* Sharp, 1884 and *C. weymarni* J. Balfour-Browne, 1947) and to occur in Japan, Korea, and eastern China (type locality) but not further to Chinese South (e.g., Guangdong) (Jiang *et al.* 2022; J. Hájek pers. com., October, 2025). In order to clarify this issue and designate a neotype of *A. zimmermanni*, it is crucial to collect new material of the species from Zhejiang, especially Hangzhou. Therefore, at present, we postulate the problem, leave it open to future study, and treat all Japanese specimens as *A. zimmermanni.*

Fig. 4. *Austrelatus zimmermanni* (Gschwendtner, 1934) comb. nov. **A–G**. Median lobe in left lateral view. **H–N**. Median lobe in right lateral view. **O, Q, S**. Right paramere. **P, R, T**. Left parameres. **A, H, O–P**. *A. z. miyakoensis* Watanabe, Kato & Shaverdo subsp. nov., holotype, Miyako-jima Island (EUMJ). **B, I, Q–R**. *A. z. daitoensis* Watanabe, Kato & Shaverdo subsp. nov., paratype, Minamidaitô-jima Island (IIM). **C–G, J–N, S–T**. *A. z. zimmermanni.* Origins: Kakeroma-jima Island (IIM) (C, J); Tanega-shima Island (IIM) (D, K); Fukuoka Prefecture (IIM) (E, L); Yamaguchi Prefecture (AAC) (F, M); Akita Prefecture (OMHM) (G, N, S–T).

Distribution in Japan of *Austrelatus zimmermanni* (Gschwendtner, 1934)

Austrelatus zimmermanni is widely distributed in Japan (Fig. 6). It is known from four administrative regions, being absent in Hokkaido, Kantô, Kansai, and Shikoku, and is collected the most in the Kyushu

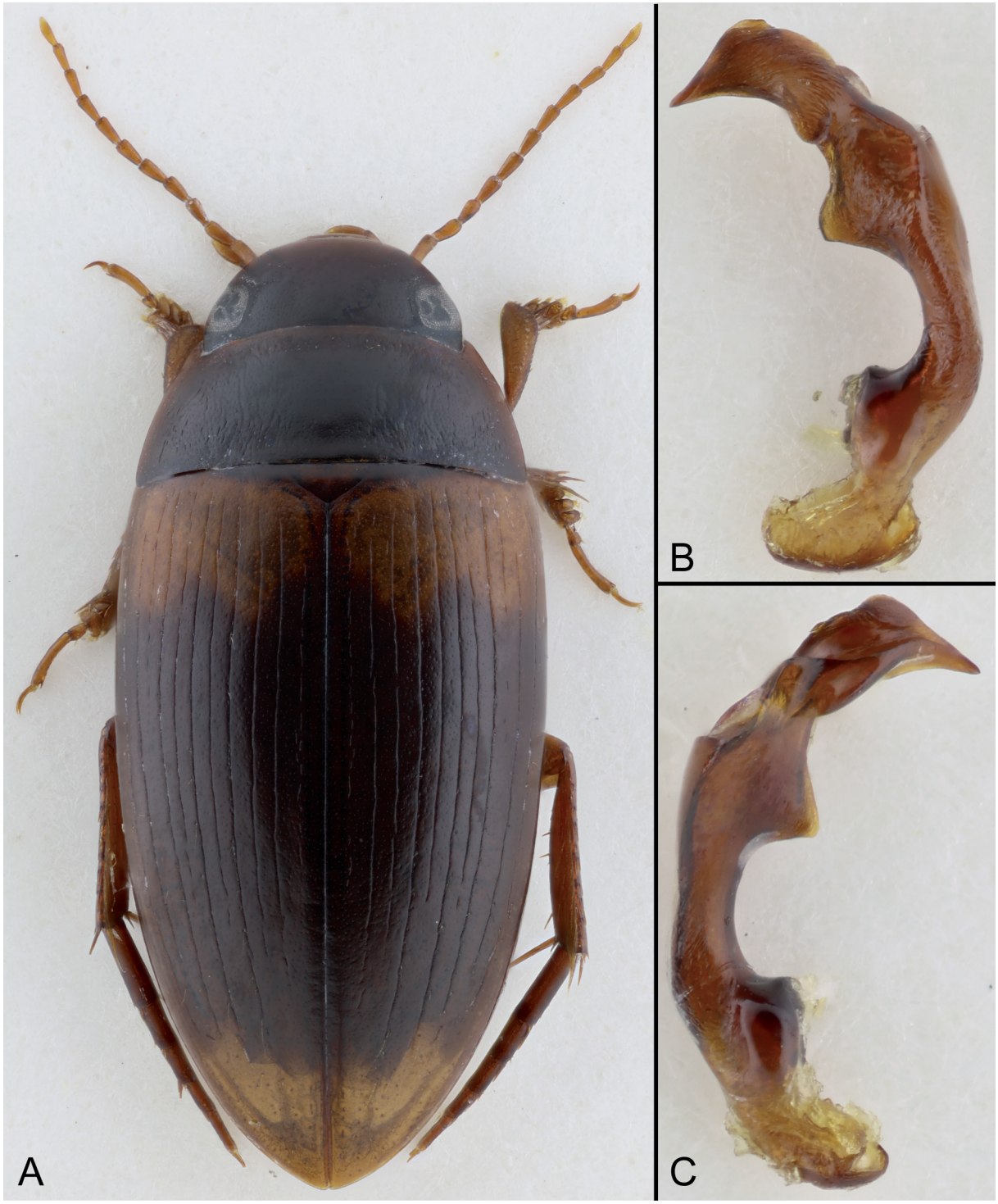

Fig. 5. Males identified as *Austrelatus zimmermanni* (Gschwendtner, 1934) comb. nov., South China (Guangdong) (NMPC). **A**. Habitus in dorsal view. **B**. Median lobe in left lateral view. **C**. Median lobe in right lateral view.

Region. Below, we provide the records in the regions and provinces according to the literature data and the studied material.

Tôhoku Region, Akita Prefecture: Sakurai (1992: 21), this study (Kisakata-machi); Takahashi (1994: 5), Satô (2004: 8) (Akita-shi, Oga Peninsula).

Chûbu Region, Nagano Prefecture (first record): this study.

Tôkai Region, Shizuoka Prefecture: Tahira & Kitano (2000: 44), this study (Nirayama-cho). Mie Prefecture: Narukawa *et al*. (2006: 99) (Kihoku-cho).

Chûgoku Region, Yamaguchi Prefecture: Aimoto (2018: 27) (Shimonoseki-shi).

Kyushu Region, Fukuoka Prefecture: Nakajima & Inoue (2004: 14) (Fukuoka-shi), this study (Kotake-machi). Saga Prefecture. Nomura *et al*. (1996: 251). Nagasaki Prefecture: Satô (1983: 37; 1985: 65) (Gotô), Fukagawa (2015: 32), Fukagawa *et al*. (2016: 22) (Nishisonogi Peninsula), Watanabe & Ohba (2022: 1) (Isahaya-shi). Tsushima Island: Satô (1998: 9), this study (Tsushima-shi). Kumamoto Prefecture: (Matsui 1987: 5) (Aso-gun), Ôtsuka (1991: 39) (Amakusa Islands). Ôita Prefecture: Miyake (2021: 100) (Yufu-shi). Miyazaki Prefecture: Iwasaki & Kinoda (1995: 106) (Miyazaki-shi, Sadowara-cho, Kiyotake-cho), this study (Kushima-shi). Kagoshima Prefecture: Matsui *et al*. (1988: 75), Imasaka *et al*. (2021: 72) (Kamikoshiki-shima, Nakakoshiki-shima islands). Yaku-shima Island: (Satô 1998: 9). Tanega-shima Island: Matsui (1988: 6), Nakamine & Nakamine (2021: 3), this study (Minamitane-cho),

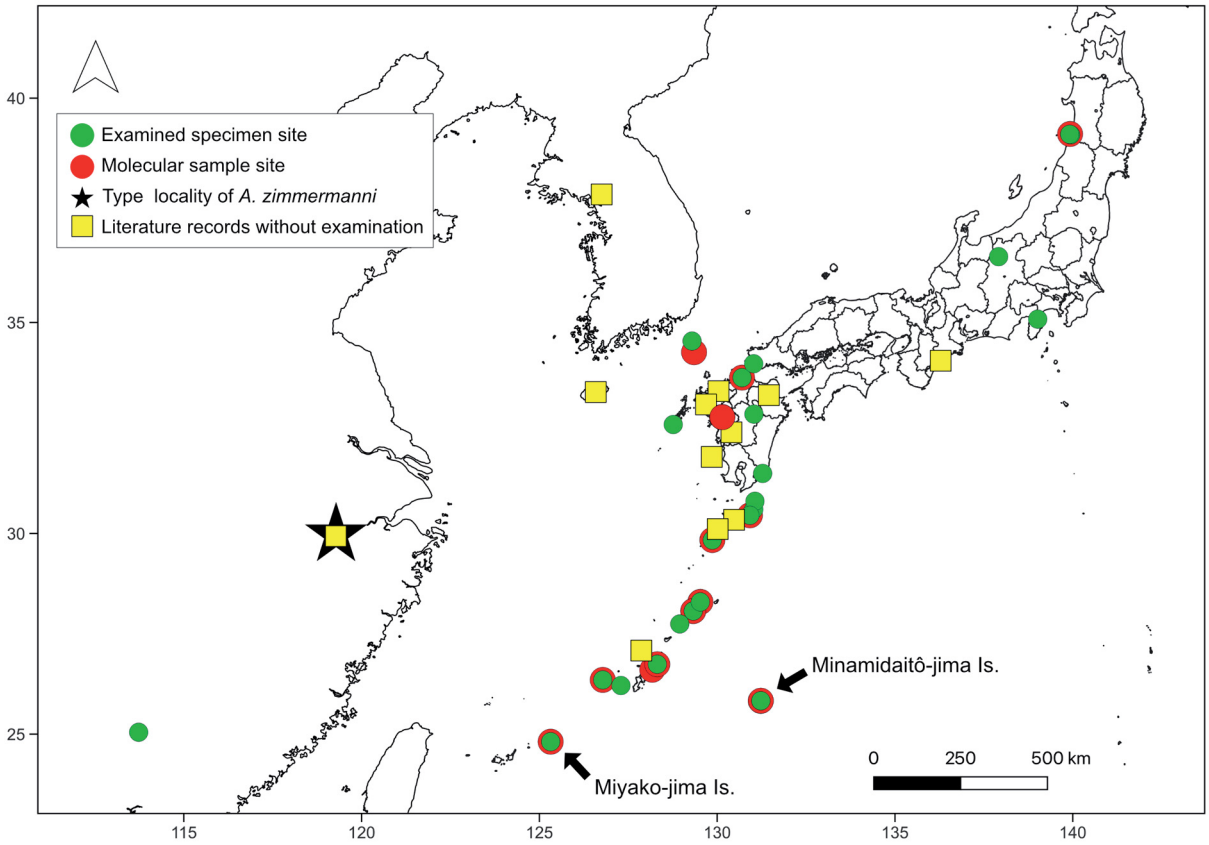

Fig. 6. Distribution map and sampling locations of *Austrelatus zimmermanni* (Gschwendtner, 1934) comb. nov.

this study (Nakatane-cho, Nishinoomote-shi). Kuchino-shima Island: Hosoya & Tanahashi (2017: 15). Nakano-shima Island: Satô (1983: 37; 1985: 65), Hosoya *et al*. (2009: 7), this study. Amami-ôshima Island: Morii (2018: 5), this study. Kakeroma-jima Island: Kato & Watanabe (2025b). Tokuno-shima Island (first record): this study. Okinoerabu-jima Island: Matsui *et al*. (1988: 75). Okinawa Prefecture, Iheya-jima Island: Aoyagi *et al*. (2022: 118). Okinawa-jima Island: Aoyagi *et al*. (2022: 118), this study. Kume-jima Island: (Matsui 1989: 20), this study. Zamami-jima Island: Kato & Watanabe (2025a: 3). Aka-jima Island: Kamite *et al*. (2019: 22). Minamidaitô-jima Island: Kamite (2003: 12), this study. Miyako-jima Island: this study.

Infraspecific structure of *Austrelatus zimmermanni* (Gschwendtner, 1934)

In Japan, *Austrelatus zimmermanni* shows a certain variability in the striation of the elytron and the dorsal colouration. Usually, with stria 9 completely reduced, its elytron has 10 dorsal striae: striae 1 (near suture), 3, 5, and 7 are frequently interrupted (Fig. 1A). Sometimes stria 7 is also strongly vestigial or completely reduced so that the elytron has only 9 striae. Seldom, stria 9 is present, though rudimentally, and therefore the elytron is with its complete striae number – 11. All striae are reduced near the apex; a

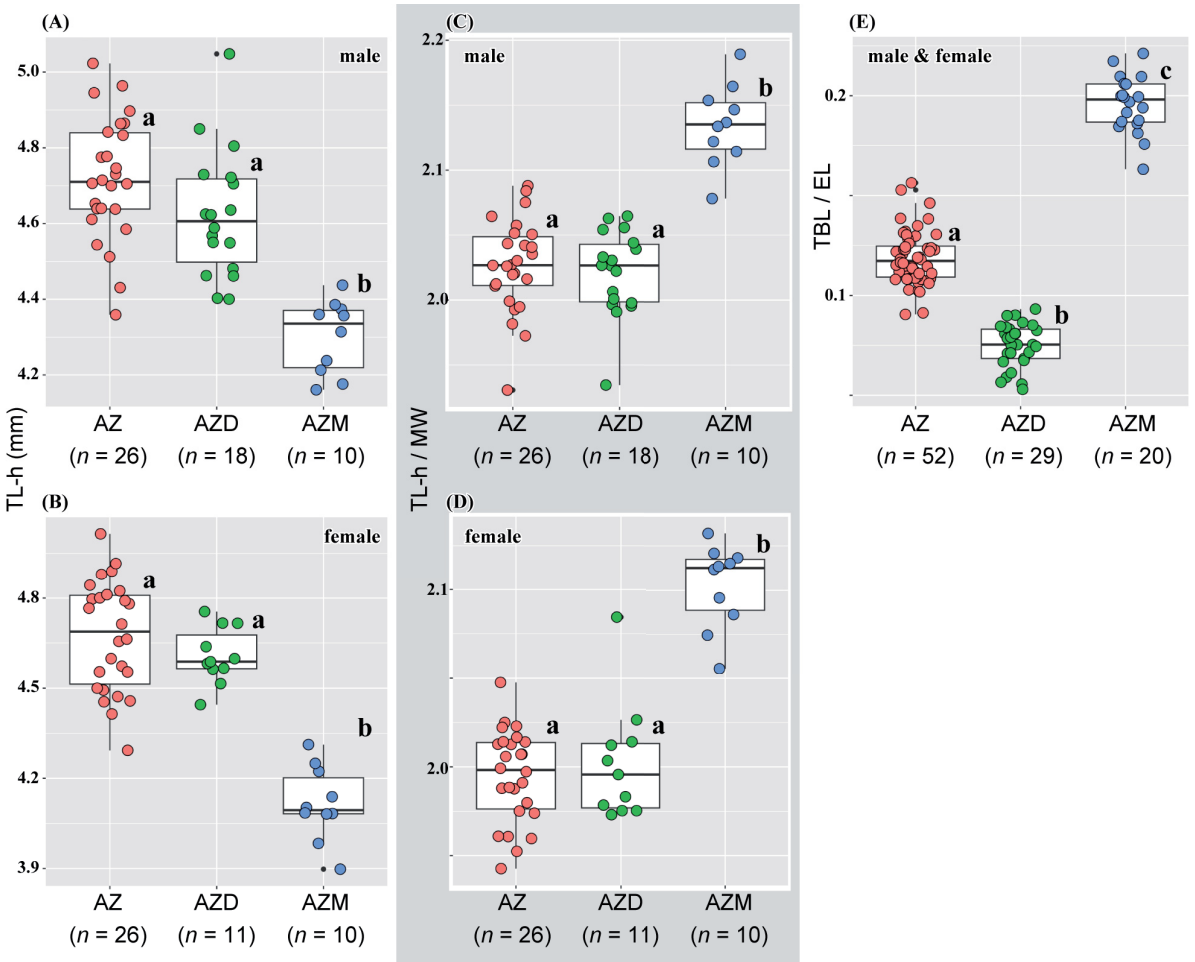

Fig. 7. Comparison of measurements among three subspecies. **A–B**. TL-h. **C–D**. TL-h/MW. **E**. TBL/EL. Abbreviations: AZ = *Austrelatus zimmermanni zimmermanni* (Gschwendtner, 1934) comb. nov.; AZD = *A. z. daitoensis* Watanabe, Kato & Shaverdo subsp. nov.; AZM = *A. z. miyakoensis* Watanabe, Kato & Shaverdo subsp. nov. Different lowercase letters (a–c) indicate significant differences (Tukey-Kramer test, $P < 0.001$ (A–B); Wilcoxon rank-sum test, $P < 0.001$ (C–E).

submarginal stria is always absent. The lateral sides of the pronotum have a reddish yellow colouration, differently developed: from present almost only at the anterolateral angles to much broader bands reaching the posterolateral angles. The elytral reddish yellow basal band varies in its width (Fig. 1A). However, populations from the Okinawa Prefecture, namely from Minamidaitô-jima and Miyako-jima islands, have much more prominent differences in their external morphology which suggest that the species has a certain infraspecific structure in the southern parts of Japan, which is most likely caused by the island isolation.

The three subspecies differ also morphometrically, supporting our visual observations in differences of the habitus shape and width of the elytral basal band, i.e., in TL-h, TL-h/MW, and TBL/EL. One-way ANOVA detected significant differences in TL-h among the three subspecies (male: $F_{2, 51} = 26.49$, $P < 0.001$; female: $F_{2, 44} = 47.08$, $P < 0.001$). The TL-h of *Austrelatus z. miyakoensis* subsp. nov. was significantly shorter than that of the nominotypical subspecies (Tukey-Kramer test, male: $P < 0.001$; female: $P < 0.001$) and *Austrelatus z. daitoensis* subsp. nov. (Tukey-Kramer test, male: $P < 0.001$; female: $P < 0.001$) (Fig. 7). No significant differences were detected between the nominotypical subspecies and *Austrelatus z. daitoensis* (Tukey-Kramer test, male: $P = 0.11$; female: $P = 0.48$) (Fig. 7). The Kruskal-Wallis tests revealed significant differences in TL-h/MW across the three subspecies (male: $\chi^2 = 23.7$, df = 2, $P < 0.001$; female: $\chi^2 = 22.7$, df = 2, $P < 0.001$). The TL-h/MW ratio was significantly higher in *Austrelatus z. miyakoensis* than in the nominotypical subspecies (Wilcoxon rank-sum test, male: $P < 0.001$; female: $P < 0.001$) and *Austrelatus z. daitoensis* (Wilcoxon rank-sum test, male: $P < 0.001$; female: $P < 0.001$) (Fig. 7). No significant differences were observed between the nominotypical subspecies and *Austrelatus z. daitoensis* (Wilcoxon rank-sum test, male: $P = 0.73$; female: $P = 0.88$) (Fig. 7). The Kruskal-Wallis tests also indicated significant differences in TBL/EL among the three subspecies ($\chi^2 = 83.0$, df = 2, $P < 0.001$). The TBL/EL ratio was significantly higher in *Austrelatus z. miyakoensis* than in the nominotypical subspecies (Wilcoxon rank-sum test: $P < 0.001$) and *Austrelatus z. daitoensis* (Wilcoxon rank-sum test: $P < 0.001$), and was significantly lower in *Austrelatus z. daitoensis* than in the nominotypical subspecies (Wilcoxon rank-sum test: $P < 0.001$) (Fig. 7).

Austrelatus zimmermanni zimmermanni (Gschwendtner, 1934) comb. nov.
Figs 1A, D, G, 4C–G, J–N, S–T

Material examined

JAPAN – **Tôhoku Region, Akita Prefecture** • 1 ♂, 1 ♀; Kisakata-machi; 10 Jun. 1992; M. Takahashi leg.; EUMJ • 4 ♀♀; Tanokami, Kisakata-machi; 31 May 1993; S. Sakurai leg.; OMHM • 1 ♂; Nagaoka, Kisakata-machi; 18 May 1996; N. Kino leg.; OMHM • 3 ♂♂, 2 ♀♀; same data as for preceding; 16 Sep. 2000; N. Kino leg.; OMHM. – **Chûbu Region, Nagano Prefecture** (first record) • 1 ♀; Yasaka-mura; 3 Aug. 1991; W. Miyata leg.; EUMJ. – **Tôkai Region, Shizuoka Prefecture** (Tahira & Kitano 2000: 44 (Nirayama-cho)) • 1 ♂, 1 ♀; Ôsawaike, Nirayamatada, Nirayama-cho; 7 May 2000; T. Kitano leg.; OMHM. – **Chûgoku Region, Yamaguchi Prefecture** (Aimoto 2018: 27) • 2 ♂♂, 1 ♀; Nogihama Sôgô Kôen, Nogihama, Shimonoseki-shi; 3 Aug. 2017; A. Aimoto leg.; AAC. – **Kyushu Region, Fukuoka Prefecture** – 2 ♂♂; Narazu, Kotake-machi, Kurate-gun; 26 Jun. 2024; M. Kato leg.; IIM. – **Nagasaki Prefecture** (Satô 1985: 65) • 1 ♂; Tomie, Gotô; 20 Apr. 1976; S. Morita leg.; EUMJ. – **Tsushima Island** • 1 ♀; Shitaru, Kamiagata-machi, Tsushima-shi; 6 Aug. 2025; M. Kato leg.; IIM. – **Kumamoto Prefecture** (Matsui 1987: 5) • 1 ♀; Jigoku, Tyoyou, Aso-gun; 28 Aug. 1986; E. Matsui leg.; EUMJ. – **Miyazaki Prefecture** • 1 ♂, 3 ♀♀; Kamichino, Honjô, Kushima-shi; 23 Apr. 2012; A. Aimoto leg.; AAC. – **Kagoshima Prefecture, Tanega-shima Island** • 3 ♂♂, 1 ♀; Masuda, Nakatane-cho, Kumage-gun; 22 May 2023; M. Kato leg.; IIM • 1 ♀; Hirayama, Minamitane-cho, Kumage-gun; 21 May 2023; M. Kato leg.; IIM • 1 ♂, 3 ♀♀; same data as for preceding; 9 Jun. 2025; M. Kato leg.; IIM • 4 ♂♂, 3 ♀♀; Iseki, Nishinoomote-shi; 20 May 2023; M. Kato leg.; IIM. – **Nakano-shima Island** (Satô 1985: 65) • 1 ♀; Nakano-shima, Tokara; 2027 Mar. 1976; S. Morita leg.; EUMJ • 2 ♂♂, 2 ♀♀; Nakano-shima,

Jittou-son, Kagoshima-gun; 12 Oct. 2024; M. Kato leg.; IIM. – **Amami-ôshima Island** • 4 ♂♂, 5 ♀♀; Kominato, Naze, Amami-shi; 27 Aug. 2025; M. Kato leg.; IIM. – **Kakeroma-jima Island** (Kato & Watanabe 2025b: 154) • 5 ♂♂, 4 ♀♀; Shodon, Setouchi-cho, Oshima-gun; 27 Jun. 2025; M. Kato leg.; IIM.– **Tokuno-shima Island** (first record) • 1 ♀; Mikyo, Tokuno-shima; 25 May 1995; H. Ohira leg.; EUMJ. – **Okinawa Prefecture, Okinawa-jima Island** • 1 ♂; Ada, Kunigami-son, Kunigami-gun; 6 Aug. 2024; M. Kato leg.; IIM. – **Kume-jima Island** • 1 ♂, 1 ♀; Hiyajô, Kumejima-cho, Shimajiri-gun; 5 Dec. 2025; M. Kato leg.; IIM. – **Zamami-jima Island** (Kato & Watanabe 2025a: 3) • 1 ♂, 1 ♀; Ama, Zamami-son, Shimajiri-gun; 5 Mar. 2023; M. Kato leg.; IIM.

Austrelatus zimmermanni daitoensis Watanabe, Kato & Shaverdo subsp. nov.
urn:lsid:zoobank.org:act:729F39E8-8146-4F50-B00A-54D20659B816
Figs 1B, E, H, 4B, I, Q–R

Copelatus zimmermanni – Kamite 2003: 12.

Diagnosis

Austrelatus zimmermanni daitoensis subsp. nov. differs from the nominotypical subspecies in a more blackish brown colouration, with a narrower reddish yellow basal band on the elytra, as well as in a beak-shaped apex of the median lobe slightly narrow. Comparision with *Austrelatus z. miyakoensis* subsp. nov. see below.

Etymology

The subspecies is named after the Daitô-jima Islands, to which its type locality, Minamidaitô-jima Island, belongs. The name is an adjective in the nominative singular.

Japanese name

We propose ‘Daitô-sesuji-gengorô’ as the Japanese name for this subspecies. ‘Daitô’ means the Daitô-jima Islands, to whose type locality, Minamidaitô-jima Island, it belongs, whereas ‘sesuji-gengorô’ refers to the subfamily Copelatinae in Japanese.

Type material

Holotype
JAPAN – **Okinawa Prefecture** • ♂; Shimajiri-gun, Minamidaitou-son, Ikenosawa [locality in hieroglyphs]; 25.84° N, 131.22° E; 2 Apr. 2025; Masaya Kato leg.; EUMJ.

Paratypes
JAPAN – **Okinawa Prefecture** • 3 ♂♂, 3 ♀♀; same collection data as for holotype; EUMJ • 11 ♂♂, 4 ♀♀; same collection data as for holotype; IIM • 4 ♂♂, 4 ♀♀; same collection data as for holotype; NHMW • 1 ♂, 1 ♀; Shimajiri-gun, Minamidaitou-son, Ikenosawa [locality in hieroglyphs]; 25.84° N, 131.22° E; 3 Apr. 2025; Masaya Kato leg.; IIM • 1 ♂; Minamidaitô-jima Island, Minamidaito-Vil, Ikenosawa [locality in hieroglyphs]; 6 Mar. 2003; Y. Kamite leg.; EUMJ (Kamite 2003) • 2 ♂♂, 3 ♀♀; Minamidaitô-jima Island, Ikenosawa [locality in hieroglyphs]; 3 Apr. 2025; T. Ikegami leg.; OMNH.

Type locality

Japan: Okinawa Prefecture, Daitô-jima Islands, Minamidaitô-jima Island, Ikenosawa, 25.84° N, 131.22° E.

Description

Body size and form. Beetle small or medium-sized, elongate, almost parallel sided, with dorsal surface convex.

Measurements. Male. TL 4.83–5.60 (mean ± SD = 5.12 ± 0.19) mm, TL-h 4.40–5.05 (4.62 ± 0.17) mm, MW 2.15–2.45 (2.29 ± 0.08) mm, TL/MW 2.14–2.36 (2.24 ± 0.05); PL 0.77–0.93 (0.84 ± 0.05) mm, PW 2.02–2.27 (2.15 ± 0.07) mm, PL/PW 0.37–0.41 (0.39 ± 0.01); DBE 0.88–0.95 (0.91 ± 0.02) mm, DBE/PW 0.39–0.45 (0.42 ± 0.02), TBL 0.20–0.35 (0.28 ± 0.04) mm; EL 3.63–4.12 (3.80 ± 0.13) mm; TBL/EL 0.05–0.09 (0.07 ± 0.01). Female. TL 4.94–5.24 (5.07 ± 0.10) mm, TL-h 4.45–4.76 (4.61 ± 0.09) mm, MW 2.21–2.41 (2.30 ± 0.06) mm, TL/MW 2.11–2.31 (2.20 ± 0.05); PL 0.78–0.86 (0.81 ± 0.03) mm, PW 2.03–2.20 (2.10 ± 0.06) mm, PL/PW 0.37–0.41 (0.39 ± 0.01); DBE 0.80–0.93 (0.88 ± 0.04) mm, DBE/PW 0.39–0.45 (0.42 ± 0.02), TBL 0.21–0.36 (0.29 ± 0.04) mm; EL 3.65–3.89 (3.79 ± 0.07) mm; TBL/EL 0.06–0.09 (0.08 ± 0.01). Holotype. TL 5.08 mm, TL-h 4.57 mm, MW 2.22 mm, TL/MW 2.29; PL 0.86 mm, PW 2.08 mm, PL/PW 0.41; DBE 0.92 mm, DBE/PW 0.44, TBL 0.25 mm, EL 3.71 mm; TBL/EL 0.07.

Colouration (Fig. 1B, E, H). Head piceous medially, between eyes and dark reddish brown anteriorly and posteriorly. Antennae and other head appendages yellowish brown. Pronotum piceous on disc and only slightly paler, dark reddish brown, towards lateral sides and anterior margin, with reddish yellow band on lateral sides which sometimes is relatively narrow or broadened on posterolateral angles. Elytron piceous, slightly paler laterally, with a narrow reddish yellow basal band reaching the lateral elytral margin, but not the suture, its anterior margin reaching basally and its posterior margin protrudes in two places. Venter dark reddish brown to piceous, with prosternum, metacoxal line and processes, partly abdominal ventrites slightly paler. Pro-, meso-, metalegs dark yellowish brown.

Surface sculpture. Head with distinct microreticulation and rather dense, uneven punctation (spaces between punctures 0–4 times size of punctures), punctures relatively coarse (diameter of punctures equal or slightly larger than diameter of microreticulation cells), finer anteriorly and posteriorly; head with two short strongly impressed transverse rows of setigerous punctures anteromedially to each eye forming a slight depression, anterior puncture row slightly longer than posterior one; a row of coarse setigerous punctures along inner eye margin present. Pronotum with numerous but relatively sparse strioles in lateral parts from anterior to posterior margins, strioles usually absent on disc and sparse along posterior margin medially; posterior margin with several longitudinal wrinkles; pronotum with microreticulation slightly finer and punctation distinctly sparser and finer than on head; coarse setigerous punctures form a broad, irregular row along anterior margin, pronotal sides, and lateral parts of posterior margin leaving posterolateral angles free and forming anteriorly and especially anterolaterally slight depressions; disc of pronotum with a relatively long, thin, longitudinal median scratch. Elytron with 9–10 dorsal striae due to reduction of striae 9 and 7; striae 1, 3, 5, and 7 frequently interrupted and reduced; all striae reduced near apex; submarginal stria absent; elytron with microreticulation slightly finer and punctation usually sparser and finer than on pronotum. Ventral part with fine, inconspicuous punctation, almost invisible on metaventrite and metacoxae and fine and sparse on abdominal ventrites getting more distinct on the last ones; prosternal process smooth medially (Fig. 1E); metaventrite and metacoxae with fine microreticulation; microreticulation much weaker on abdominal ventrites; metacoxal plates with numerous, distinctly impressed longitudinal strioles; abdominal ventrites 1 and 2 with numerous, long, longitudinal strioles from margin to margin, on abdominal ventrites 3–5 strioles situated laterally and turn to middle, almost horizontal, much weaker and shorter on ventrite 5; abdominal ventrite 6 without strioles or with 1–2 very fine ones; abdominal ventrites 3–5 with solitary, coarse setigerous punctures in middle baring long setae; abdominal ventrites 5 and 6 with solitary coarse setigerous punctures sublaterally, on abdominal ventrite 6 they form a very short skew row on each sublateral side (Fig. 1H).

Structures. Head broad, sub-trapezoidal, with anterior margin of clypeus slightly and evenly concave, with a distinct bead laterally on both sides. Pronotum transverse, broadest in posterior half, with lateral margins slightly convergent anteriorly, with anterior angles projecting and posterior angles

slightly rounded. Pronotal base as broad as base of elytra or slightly narrower. Pronotum with thin but distinct lateral bead missing at anterior angles. Elytron with distinct lateral bead. Base of prosternum narrowly rounded anteriorly, convex medially; neck of prosternal process convex; neck and blade of prosternal process evenly joined; blade of prosternal process lanceolate, rather short, with distinct lateral bead especially laterally and broadly pointed apex (Fig. 1E). Lateral projections of metaventrite tongue-shaped, very slender. Metacoxal lines divergent, indistinct close to metaventrite, not reaching it (Fig. 1H). Abdominal ventrite 6 beaded, broadly rounded. Male. Antennae and protibiae simple. Pro- and mesotarsomeres 1–3 distinctly broadened, with circular-shaped adhesive setae ventrally. Protarsomere 4 small, anteroventrally on each side with several long, thin setae, one of which especially strong. Protarsomere 5 long, thin, with two seta rows ventrally. Proclaws short, curved and subequal. Dorsal and ventral margins of mesotibiae and dorsal margin of mesotarsi with natatory setae; dorsal and ventral margins of metatibiae and metatarsi with natatory setae. Median lobe of aedeagus broad, stout, strongly curved, consisting mostly of strongly sclerotised dorsal sclerite, not divided into two apical lobes. Ventral sclerite small, membranous, but distinctly visible in ventral view, occupying a large, rounded ventral opening and divided into two apical lobes. Lateral sides of dorsal sclerite have complex form with different concavities and projections (Fig. 4B, I); in lateral view, left lateral side with a large, rounded concavity in middle and connected to it a large dorsal projection with broadly rounded apex; subapically, left lateral side with a large, elongate, flat crest; left ventral margin of dorsal sclerite with a deep notch subapically, better visible in right lateral and ventral views. Ventral opening more or less rounded in middle and presented as deep groove apically; its left margin strongly elevated and with a small, but deep notch. Apex beak-shaped, slightly curved downwards, with two small crests, one on tip and the other on lateral margin. Parameres narrow, subtriangular, slightly different in shape: right paramere (Fig. 4Q) with ventral margin straighter apically and with smaller but deeper concavity basally than that of left one (Fig. 4R); its dorsal margin with dense long setae; distal setae longer than proximal ones; apical lobe club-shaped. Female. Similar to males in external morphology, except for not modified pro- and mesotarsi. Most of the females have more intensive dorsal surface sculpture, e.g., with more numerous longitudinal strioles on pronotum covering sparsely also its disc, and with 10 elytral striae.

Variability. There is a variation in the colouration and dorsal striolation as described above. Holotype has 9 elytral striae.

Distribution

Japan, Kyushu Region, Okinawa Prefecture, the Nansei Islands: Minamidaitô-jima Island.

Habitat

Specimens were collected from two sites on Minamidaitô-jima Island. Both sites were wetlands within forested areas, and this subspecies was obtained from sediments along the shoreline.

Austrelatus zimmermanni miyakoensis Watanabe, Kato & Shaverdo subsp. nov.
urn:lsid:zoobank.org:act:C1C8059F-AD33-4C48-A2D0-8B01B01E4AD7
Figs 1C, F, I, 2–3, 4A, H, O–P

Diagnosis

Austrelatus zimmermanni miyakoensis subsp. nov. differs from both other subspecies in the smaller, narrower (especially in elytral part) and more elongate habitus, the absence of elytral striae, a broader reddish yellow basal band on the elytra and differences in shape of the median lobe: a more slender apex, with more weakly developed apical crests, a smaller but more prominent subapical projection of the left lateral side, and a slightly differently shaped and less twisted dorsal projection.

Etymology

The subspecies is named after its type locality, Miyako-jima Island, the largest of the Miyako Islands. The name is an adjective in the nominative singular.

Japanese name

We propose 'Sujinashi-sesuji-gengorô' as the Japanese name for this subspecies. 'Sujinashi' means 'without striae,' referring to the absence of elytral striae.

Type material

Holotype

JAPAN – **Okinawa Prefecture** • ♂; Miyakojima-shi, Hirara, Higashinakasonezoe [locality in hieroglyphs]; 24.80° N, 125.31° E; 26 Apr. 2024; Masaya Kato leg.; EUMJ.

Paratypes

JAPAN – Okinawa Prefecture • 2 ♂♂, 3 ♀♀; same collection data as for holotype; EUMJ • 3 ♂♂, 7 ♀♀; same collection data as for holotype; IIM • 1 ♂, 2 ♀♀; same collection data as for holotype; NHMW • 2 ♂♂, 1 ♀; Miyakojima-shi, Hirara, Higashinakasonezoe [locality in hieroglyphs]; 24.80° N, 125.31° E; 27 Apr. 2024; Masaya Kato leg.; IIM • 2 ♂♂, 1 ♀; same collection data as for preceding; NHMW.

Type locality

Japan: Okinawa Prefecture, Miyako Islands, Miyako-jima Island, Hirara, Higashinakasonezoe, 24.80° N, 125.31° E.

Description

Body size and form. Beetle small, distinctly elongate, narrow, subparallel sided, with dorsal surface convex.

Measurements. Male. TL 4.66–4.92 (4.79 ± 0.09) mm, TL-h 4.16–4.44 (4.30 ± 0.10) mm, MW 1.94–2.10 (2.02 ± 0.05) mm, TL/MW 2.28–2.44 (2.38 ± 0.04); PL 0.71–0.84 (0.77 ± 0.05) mm, PW 1.82–1.98 (1.91 ± 0.05) mm, PL/PW 0.36–0.43 (0.40 ± 0.02); DBE 0.92–1.00 (0.96 ± 0.03) mm, DBE/PW 0.48–0.52 (0.50 ± 0.01), TBL 0.60–0.81 (0.69 ± 0.07) mm; EL 3.42–3.65 (3.53 ± 0.08) mm; TBL/EL 0.18–0.22 (0.20 ± 0.02). Female. TL 4.33–4.80 (4.58 ± 0.13) mm, TL-h 3.90–4.31 (4.12 ± 0.12) mm, MW 1.84–2.04 (1.96 ± 0.06) mm, TL/MW 2.32–2.36 (2.34 ± 0.01); PL 0.65–0.78 (0.73 ± 0.04) mm, PW 1.74–1.90 (1.83 ± 0.05) mm, PL/PW 0.37–0.44 (0.40 ± 0.02); DBE 0.88–0.96 (0.93 ± 0.03) mm, DBE/PW 0.49–0.53 (0.51 ± 0.01), TBL 0.54–0.71 (0.66 ± 0.06) mm; EL 3.21–3.58 (3.39 ± 0.12) mm; TBL/EL 0.16–0.21 (0.20 ± 0.01). Holotype. TL 4.74 mm, TL-h 4.21 mm, MW 2.00 mm, TL/MW 2.37; PL 0.79 mm, PW 1.88 mm, PL/PW 0.42; DBE 0.93 mm, DBE/PW 0.49, TBL 0.60 mm, EL 3.42 mm; TBL/EL 0.18.

Colouration (Figs 1C, F, I, 2). Head dark reddish brown anteriorly and posteriorly and darker, almost piceous medially, between eyes. Antennae and other head appendages yellowish brown. Pronotum reddish brown to dark reddish brown, darker on disc (sometimes to piceous) and distinctly and gradually paler towards lateral sides and anterior margin, so that usually lateral sides without a distinct band but just reddish yellow, especially on anterolateral angles. Elytron reddish brown to dark reddish brown, sometimes to piceous, paler laterally, with a broad reddish yellow basal band reaching lateral elytral margin and not suture, its anterior margin reaching basally and posterior margin protrudes in two places. Venter reddish yellow to dark reddish brown, distinctly darker, to piceous, on metaventrite sublaterally and metacoxal plates (Fig. 1I). Pro-, meso-, metalegs yellowish brown.

Surface sculpture. As in previous subspecies, except for finer microreticulation and distinctly finer (diameter of punctures smaller or equal to diameter of microreticulation cells), sparser (spaces between punctures 0–3 times size of punctures) and more even punctation on pronotum, elytron and especially on head. Pronotum without strioles and longitudinal wrinkles. Elytron without striae, but with four lines of setigerous punctures, second and fourth puncture lines inconspicuous, with punctures spaced. Metacoxal plates and abdominal ventrites 1, 3–6 without longitudinal strioles (Fig. 1I), on basal ventrite 2 strioles much weaker and shorter.

Structures. As in previous subspecies, except for pronotal base as broad as base of elytra or slightly broader. Due to subparallel sides of elytra, pronotum sometimes broader than elytron. Male. As in previous subspecies, except for more slender apex of median lobe, with more weakly developed apical crests, smaller but more prominent subapical crest of left lateral side, slightly differently shaped and less twisted dorsal projection (Fig. 4A, H). Female. Similar to males in external morphology, except for not modified pro- and mesotarsi. Body size smaller than that of male.

Variability. There is a variation in the colouration as described above. Holotype has colouration reddish brown, with a broad, reddish yellow basal band nearly reaching elytral suture (Fig. 1C).

Distribution

Japan, Kyushu Region, Okinawa Prefecture, the Nansei Islands: Miyako-jima Island.

Habitat

Specimens were collected from a single site on Miyako-jima Island—a wetland within a forest that becomes flooded by rainwater and dries out during the summer drought. This subspecies was obtained from sediments along the shoreline.

Biology and phenology of Austrelatus zimmermanni (Gschwendtner, 1934)

Austrelatus zimmermanni inhabits ponds with stable water levels (Tahira & Kitano 2000; Nakajima & Inoue 2004; Aimoto 2018) and ephemeral rain pools prone to drying (Watanabe & Ohba 2022), including rice paddies in the open plains (Han *et al*. 2011). In Japan, *A. z. zimmermanni* inhabits vegetated zones of plant-rich ponds (Mitamura *et al*. 2017; Nakajima *et al*. 2020), whereas *A. z. daitoensis* subsp. nov. and *A. z. miyakoensis* subsp. nov. inhabit aquatic habitats surrounded by forests with sparse vegetation. According to the material examined, adults of *A. zimmermanni* are known to be collected in the spring (March, April, and May) and summer (June, July, and August). In the literature sources, adults are reported in spring (March) to autumn (October) (e.g., Takahashi 1994; Mitamura *et al.* 2017). Larvae have not been observed in the field since the adult insects collected on May 31st laid eggs on June 7th, the breeding season is thought to be early summer (Watanabe & Ohba 2022). In addition, *A. zimmermanni* appears to undergo emergence in late summer, as evidenced by collections of new adults in August and September (Sato 2004; Aimoto 2018). Adults are known to fly to light traps (Ôtsuka 1991; Sato 2004). Watanabe & Ohba (2022) studied the life history of the species and suggested that its larval period is shorter than that of other species of *Copelatus*, which enables it to inhabit highly ephemeral aquatic habitats. In fact, this species is often found in small, temporary water pools that dry up easily. The larvae feed by swallowing live chironomid larvae and Tubificina (Watanabe & Ohba 2022).

Our examination of the life cycle of *Austrelatus z. miyakoensis* subsp. nov. showed that in the field, adult mating took place at the type locality in April. In captivity, the first eggs (Fig. 3A) were found on 14 June 2024, 20 days after adult collection. The eggs were laid singly and adhered to the Java moss surface, similar as observed in other species of *Austrelatus* and *Copelatus* (e.g., Watanabe *et al*. 2017, 2024; Watanabe 2025). The egg period lasted 3–7 days (5.3 ± 1.1 days, n = 19). The total larval period

was 21–44 days (30.8±6.6 days, n = 15): first instar larvae (Fig. 3C), 5–12 days (6.1±2.1 days, n = 18); second instar larvae (Fig. 3D), 5–20 days (12.0±4.8 days, n = 16); and third instar larvae (Fig. 3E), 11–16 days (12.7±1.3 days, n = 15). All larvae captured live chironomid larvae and Tubificina Brinkhurst & Jamieson, 1971 using their mandibles and swallowed prey whole, consuming from the hatching and

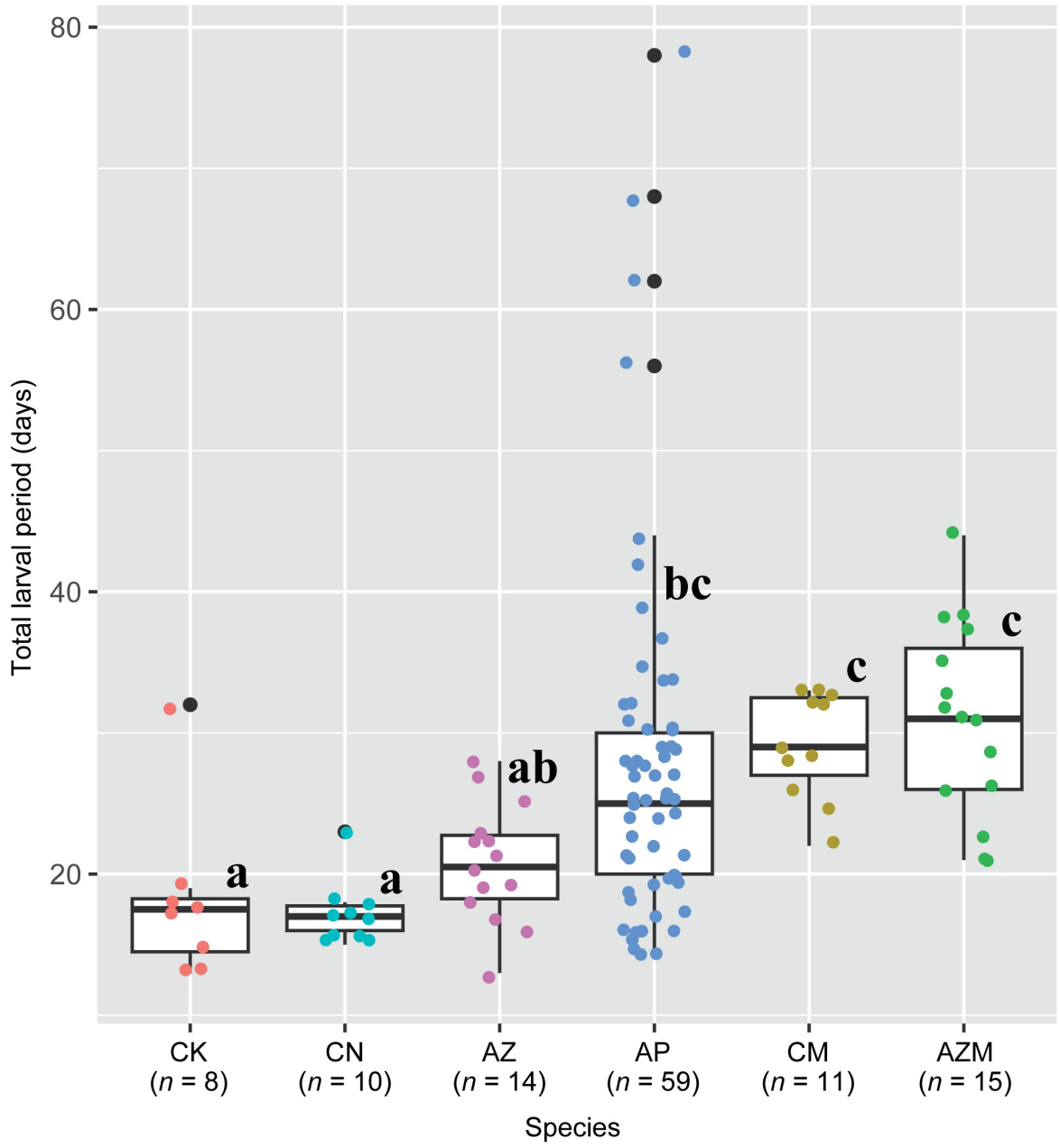

Fig. 8. Comparison of total larval period among five species and one subspecies of Copelatinae. Abbreviations: AP = *A. parallelus* (Zimmermann, 1920); AZ = *Austrelatus zimmermanni zimmermanni* (Gschwendtner, 1934) comb. nov.; AZM = *A. z. miyakoensis* Watanabe, Kato & Shaverdo subsp. nov.; CK= *Copelatus kammuriensis* Tamu & Tsukamoto, 1955; CM = *C. masculinus* Régimbart, 1899; CN = *C. nakamurai* Guéorguiev, 1970; Different lowercase letters indicate significant differences according to Wilcoxon rank-sum test ($P<0.05$). CK, CN, AZ, AP, and CM used datasets reported by Watanabe *et al.* (2017, 2024), Watanabe & Hayashi (2019), Watanabe (2022), Watanabe & Ohba (2022).

moulting day onward. After transitioning to land within the pupal cups, the larvae dug into the soil and constructed a pupal chamber. The period of the pupal stage could not be determined because in all pupation cups, the inside of the pupal chamber could not be observed from outside the cup. The period from landing to emergence was 10–12 days (11.2 ± 0.6 days, n = 12). All new adults escaped from the pupal chamber on their own after emergence (Fig. 3B). The complete developmental period was 35–61 days (47.3 ± 6.9 days, n = 12). The body of newly emerged adults was coloured, but compared to the wild adults, the abdomen was slightly lighter.

Comparison of larval periods among five species of *Copelatinae*

A Kruskal-Wallis test showed a significant difference in the total larval period among the five species and one subspecies ($\chi^2 = 37.96$, $df = 5$, $P < 0.001$). The total larval period was significantly longer for *Austrelatus z. miyakoensis* subsp. nov. than for *C. kammuriensis*, *C. nakamurai*, and *A. z. zimmermanni* (Wilcoxon rank-sum test: $P < 0.01$), for *C. masculinus* than for *C. kammuriensis* (Wilcoxon rank-sum test: $P < 0.05$), *C. nakamurai*, and *A. z. zimmermanni* (Wilcoxon rank-sum test: $P < 0.01$), for *A. parallelus* than for *C. kammuriensis* (Wilcoxon rank-sum test: $P < 0.05$) and *C. nakamurai* (Wilcoxon rank-sum test: $P < 0.01$) (Fig. 8). However, no significant difference was observed in the total larval periods

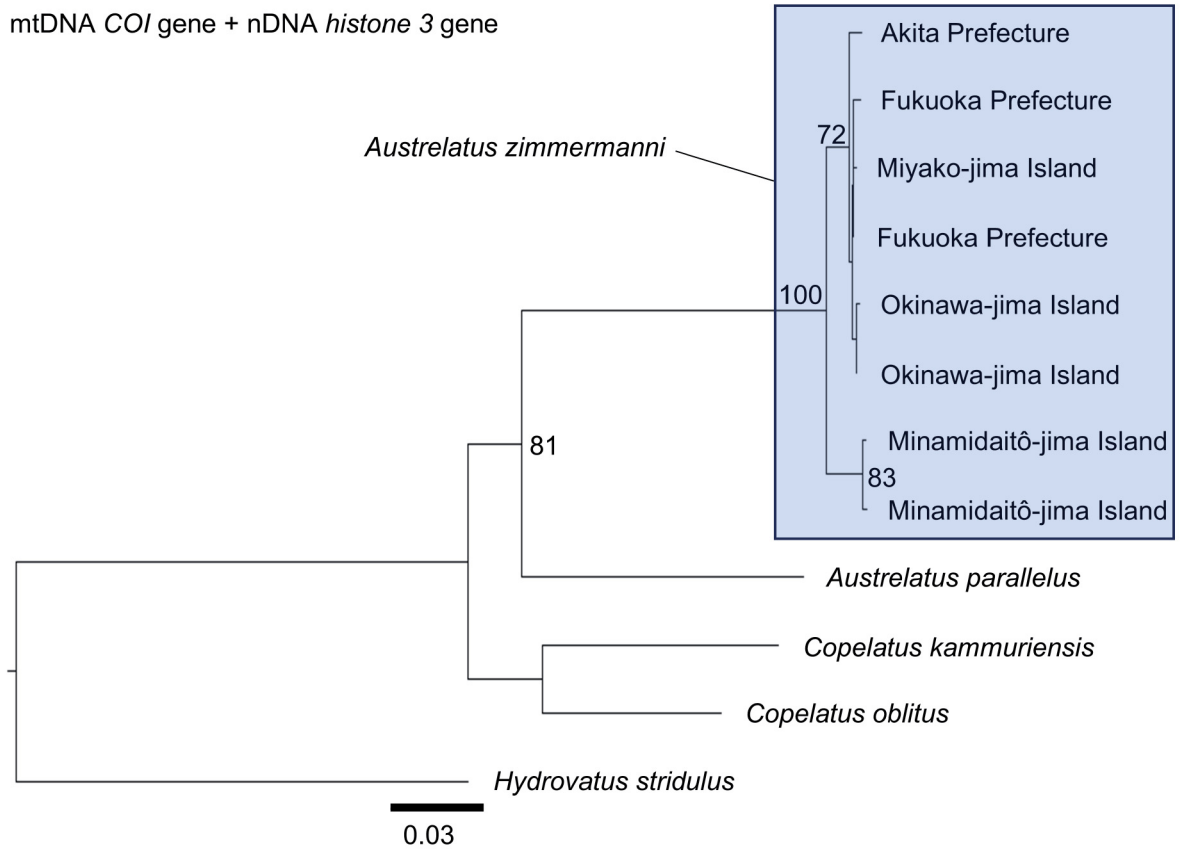

Fig. 9. Maximum likelihood phylogenetic tree based on the dataset 1 (599 bp of the mitochondrial *COI* gene and 301 bp of the nuclear *histone 3* gene). The area enclosed by the blue rectangle represents specimens of *Austrelatus zimmermanni* (Gschwendtner, 1934) comb. nov. collected in Japan. The values near the nodes of the phylogenetic tree are the ultrafast bootstrap values, and they are shown when the values are 70 or higher.

of *C. kammuriensis*, *C. nakamurai*, and *A. z. zimmermanni*; *A. z. zimmermanni* and *A. parallelus*; *A. parallelus*, *C. masculinus* and *A. z. miyakoensis*, respectively (Fig. 8).

Phylogenetic analysis based on the mtDNA and the nDNA

The ML tree based on the dataset 1 (mtDNA *COI* gene 599 bp and the nDNA *histone 3* gene 301 bp) indicated that specimens of *Austrelatus zimmermanni* from Japan formed a clade with a high ultrafast bootstrap value of 100. In addition, no genetic differentiation was observed among them, except for the Minamidaitô-jima Island population. The species did not form a clade with *Copelatus* but with *A. parallelus*, and the ultrafast bootstrap value was 81 (Fig. 9). In the dataset 2 (*COI* gene 599 bp), *A. zimmermanni* clade was also strongly supported with a high ultrafast bootstrap value of 100. Although the clade formed a monophyletic clade with *A. parallelus*, the ultrafast bootstrap value was low (<70) (Supp. file 1). Because no nucleotide substitutions were detected within *A. zimmermanni* in the nDNA *histone 3* gene, it was excluded from subsequent analyses.

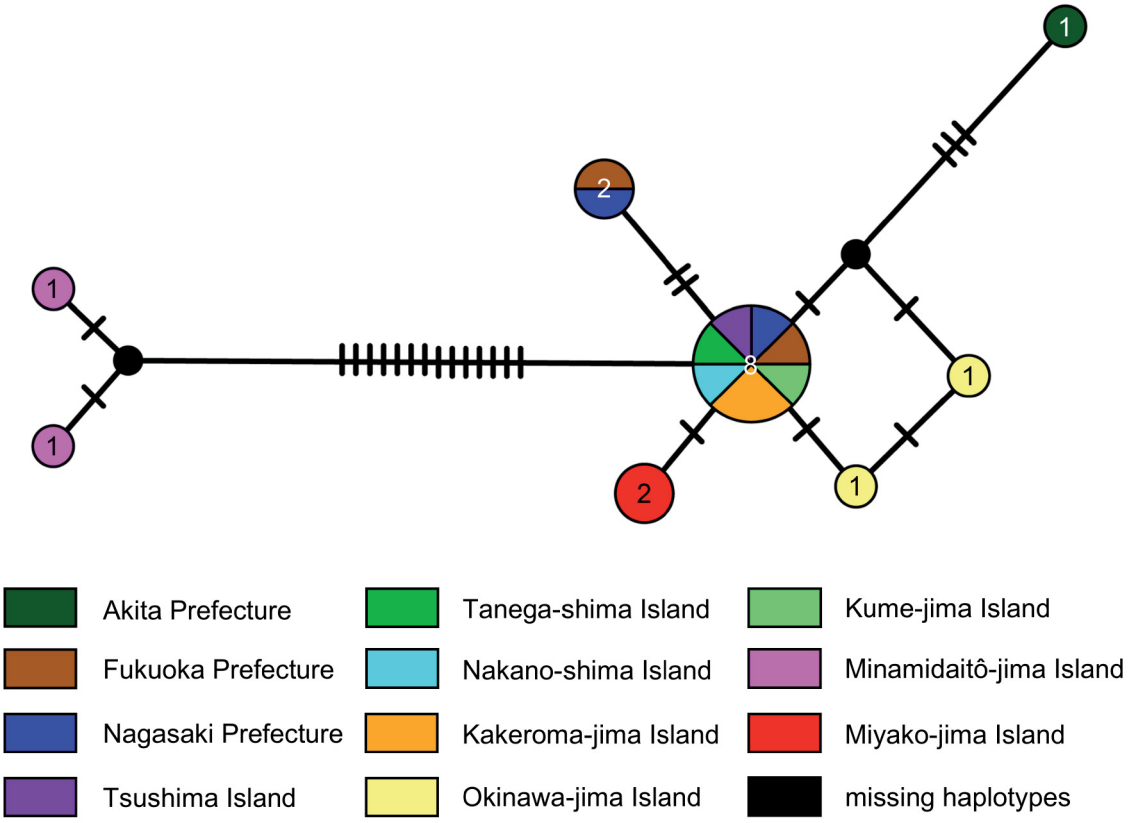

Fig. 10. Haplotype network based on 599 bp of the mitochondrial *COI* gene from 17 samples of *Austrelatus zimmermanni* (Gschwendtner, 1934) comb. nov. collected in Japan. Each circle represents a haplotype, and the numbers inside the circles represent the sample sizes. Line distance between circles corresponds to the number of nucleotide differences, and vertical bars along lines represent the number of nucleotide substitutions between haplotypes. Black circles without the number of sample sizes represent missing haplotypes. The colors in the haplotype network correspond to the colors of the sampling sites below the network.

Table 1. Genetic distances (pairwise distances) between haplotypes of the mitochondrial DNA *COI* gene.

Sampling sites	Akita	Fukuoka	Fukuoka	Okinawa-jima	Okinawa-jima	Minamidaitô-jima	Minamidaitô-jima	Miyako-jima
Akita	–	–	–	–	–	–	–	–
Fukuoka	0.0101	–	–	–	–	–	–	–
Fukuoka	0.0067	0.0034	–	–	–	–	–	–
Okinawa-jima	0.0067	0.0067	0.0034	–	–	–	–	–
Okinawa-jima	0.0084	0.0050	0.0017	0.0017	–	–	–	–
Minamidaitô-jima	0.0285	0.0285	0.0251	0.0285	0.0268	–	–	–
Minamidaitô-jima	0.0285	0.0285	0.0251	0.0285	0.0268	0.0034	–	–
Miyako-jima	0.0084	0.0050	0.0017	0.0050	0.0034	0.0268	0.0268	–

The median-joining haplotype network based on the mtDNA *COI* gene 599 bp showed that 8 haplotypes were observed within 11 populations (Fig. 10). Seven sites in Kyushu and the Nansei Islands were included in the major haplotype, and samples collected from Akita Prefecture and Okinawa-jima Island each possessed unique haplotypes. The Miyako-jima Island population differed from the major haplotype by a single nucleotide substitution and possessed a unique haplotype. The Minamidaitô-jima Island population was highly genetically differentiated compared with other populations. The pairwise genetic distances of the mtDNA *COI* gene between the Minamidaitô-jima Island population and the other

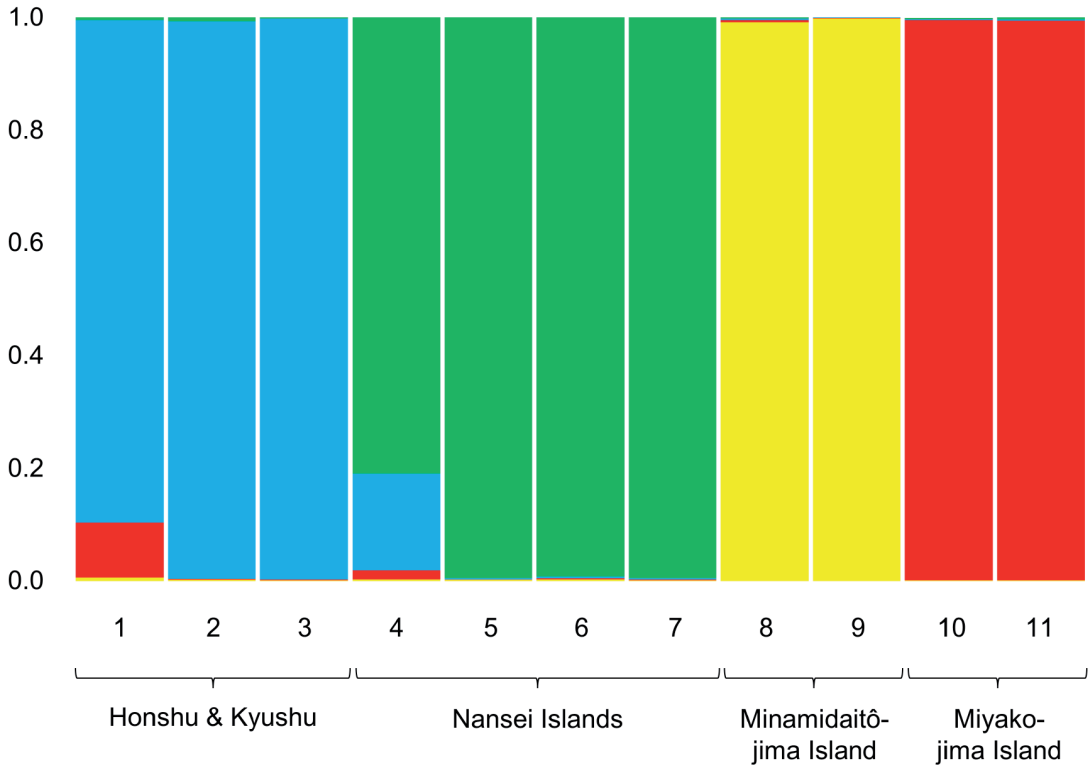

Fig. 11. Genetic structure selected as the optimal *K* (*K* = 4) based on the 166 SNPs data from 11 samples of *Austrelatus zimmermanni* (Gschwendtner, 1934) comb. nov. collected in Japan. The Y-axis represents proportions ranging from 0 to 1. Each column represents one individual; 1 = Akita Prefecture; 2–3 = Fukuoka Prefecture; 4 = Nakano-shima Island; 5 = Kakeroma-jima Island; 6–7 = Okinawa-jima Island; 8–9 = Minamidaitô-jima Island; 10–11 = Miyako-jima Island.

populations ranged from 2.51 to 2.85%, whereas the genetic distances between the Miyako-jima Island population and the populations excluding the Minamidaitô-jima Island population ranged from 0.17 to 0.84 % (Table 1).

Molecular analysis based on the MIG-seq dataset

In the genetic structure analysis based on the 166 SNPs data using STRUCTURE ver. 2.3.4., $K = 4$ was selected as the optimal K, due to the highest ΔK value. At $K = 4$, the populations were separated into Honshu and Kyushu cluster and the Nansei Islands cluster (Nakano-shima, Kakeroma-jima, and Okinawa-jima Islands) and Minamidaitô-jima Island cluster, and Miyako-jima Island cluster (Fig. 11). The morphologically distinct Minamidaitô-jima Island and Miyako-jima Island populations were not included in the Nansei Islands cluster, geographically adjacent to those two populations (Fig. 11). Phylogenetic tree, estimated from the same dataset, indicated a trend similar to the result of the genetic structure analysis using STRUCTURE ver. 2.3.4., separated into four groups (Fig. 12). The branch length of the Minamidaitô-jima Island population was long, indicating highly genetically differentiated compared with other populations. In contrast, the branch lengths among the remaining populations were similar, suggesting the same levels of genetic differentiation.

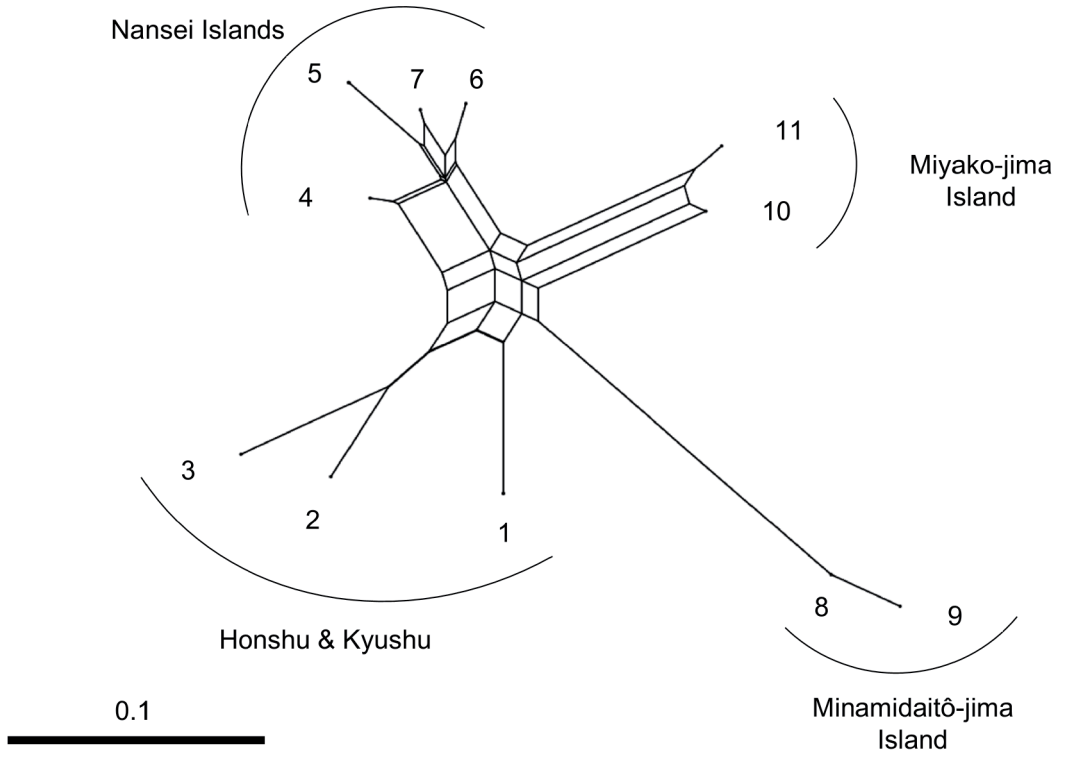

Fig. 12. Phylogenetic tree using the neighbor-net method based on the 166 SNPs data from 11 samples of *Austrelatus zimmermanni* (Gschwendtner, 1934) comb. nov. collected in Japan. The number represents one individual; 1 = Akita Prefecture; 2–3 = Fukuoka Prefecture; 4 = Nakano-shima Island; 5 = Kakeroma-jima Island; 6–7 = Okinawa-jima Island; 8–9 = Minamidaitô-jima Island; 10–11 = Miyako-jima Island.

Discussion

As a result of the morphological examination, *Copelatus zimmermanni* is considered to belong to the genus *Austrelatus*, as supported by the morphology of the male genitalia. This relationship is also suggested by the topology of the ML trees based on the dataset 1 (the mtDNA *COI* gene and the nDNA *histone 3* gene) and the dataset 2 (the mtDNA *COI* gene) showed that *A. zimmermanni* did not form a clade with *Copelatus* but formed a sister group instead with *A. parallelus* (Fig. 9, Supp. file 1). However, the number of samples from both genera used in this study is limited. Therefore, further molecular phylogenetic analyses with increased sampling from both genera are necessary to examine their taxonomic placement in detail.

The haplotype network based on the mtDNA *COI* gene and genetic structure analyses using genome-wide SNPs revealed that the morphologically distinct populations of *A. zimmermanni* from Minamidaitô-jima Island and Miyako-jima Island are genetically differentiated from the other populations (Figs 10–12). The Minamidaitô-jima Island population shows a highly genetic differentiation from the other populations (Figs 10, 12), which is consistent with the results of the analyses based on the mtDNA *COI* gene and genome-wide SNPs. In addition, the haplotype network based on the mtDNA *COI* gene revealed that the Miyako-jima Island population possessed a unique haplotype by one nucleotide substitution from the major haplotype (Fig. 10), and the results based on the genome-wide SNPs showed clear genetic differentiation from the other populations (Figs 11–12). The MIG-seq method detects SNPs from ISSR regions (Suyama & Matsuki 2015), which are genomic regions flanked by SSR regions that are considered to have a rapid evolutionary rate. Therefore, these results likely reflect the detection of genome-wide mutations that accumulated more rapidly than nucleotide substitutions in the mtDNA *COI* gene after the Miyako-jima Island population became isolated from the other populations. Based on these findings, the Minamidaitô-jima Island and Miyako-jima Island populations are unlikely to experience gene flow from the other populations. These two populations also possess unique morphological characteristics. The absence of elytral striae in the Miyako-jima Island population was observed in all field-collected specimens and in all subsequent generations in the laboratory. Furthermore, an ecological difference was observed: the larval period of the Miyako-jima Island population was significantly longer than that of the Kyushu population (Fig. 8). Therefore, we argue that it is reasonable to treat them as separate subspecies.

The evolutionary rate of the *COI* gene in Coleoptera has been estimated at approximately 1.77% per million years (Ma) (Papadopoulou *et al*. 2010). Phylogenetic analysis based on the mtDNA *COI* gene indicated that the Minamidaitô-jima Island population shows a genetic distance of 2.51–2.85% compared to other populations (Table 1), indicating that it has been isolated for approximately 1.42–1.61 Ma. Although the Daitô Islands are oceanic islands and have never been connected to a continent or other islands, they share species with the Nansei Islands, some of which have subspecies endemic to the Daitô Islands, such as *Pteropus dasymallus daitoensis* Kuroda, 1921, *Otus elegans interpositus* Kuroda, 1923, and *Euterpnosia chibensis daitoensis* Matsumura, 1917. In addition, the terrestrial snail *Bradybaena circulus circulus* (Pfeiffer, 1846) shows a genetic relationship between populations from Okinawa-jima Island and its adjacent islands and those from the Daitô Islands, suggesting dispersal by ocean currents (Hirano *et al*. 2014). Similarly, individuals of *A. zimmermanni* inhabiting Okinawa-jima Island or other islands of the Nansei Islands may have been washed out to the Pacific Ocean by typhoons or other events and subsequently reached Minamidaitô-jima Island via ocean currents.

In contrast, the Miyako-jima Island population shows a genetic distance of 0.17–0.84% in the mtDNA *COI* gene compared to other populations (excluding the Minamidaitô-jima Island population) (Table 1), suggesting more recent isolation. Some species inhabiting Miyako-jima Island have been known to be phylogenetically closely related to congeneric species or conspecific populations from the Okinawa Islands, e.g., *Hebius concelarus* (Malnate, 1963) (Kaito & Toda 2016) and *Microhyla okinavensis*

Stejneger, 1901 (Matsui & Tominaga 2020). One possible explanation is the hypothesis that the Okinawa–Miyako Submarine Plateau (OMSP) once existed as land bridge and served as a migration corridor from the Okinawa Islands to Miyako-jima Island (Watanabe *et al*. 2023). The genetic distance of 0.34–0.50% between the Miyako-jima Island and Okinawa-jima Island populations suggests that they became isolated approximately 0.19–0.28 Ma, based on the mtDNA *COI* evolutionary rate reported by Papadopoulou *et al*. (2010). The OMSP may have remained emergent until 0.27 Ma (Watanabe *et al*. 2023), and this estimated age is consistent with that evidence. Thus, it is possible that the Miyako-jima Island population became completely isolated from other populations when the OMSP submerged. In other words, the Miyako-jima Island population may represent an early stage of speciation, in which morphological variation arose before detectable changes accumulated in the mtDNA *COI* gene. This pattern resembles that observed in *Acilius japonicus* Brinck, 1939, and *A. kishii* Nakane, 1963, in which *A. kishii* is thought to have been isolated from other *A. japonicus* populations after the last glacial period. In both species, variation in the elytra arose before detectable differences in male genitalia or the mtDNA *COI* gene (Bergsten & Miller 2007).

Austrelatus zimmermanni is widely distributed from northern to southern Japan. In populations other than *A. z. miyakoensis* subsp. nov., the elytra are with 9–11 dorsal striae, whereas *A. z. miyakoensis*, distributed at the southernmost limit of the species range, lacks elytral stria. Similar cases have been confirmed in some other Japanese Dytiscidae. *Acilius kishii* was described as a subspecies of *A. japonicus* based on the characteristic of indistinct grooves on the female elytra compared to *A. japonicus* (Nakane 1963) and was later elevated to species (Satô 1984). Within the distributional range encompassing *A. japonicus* and *A. kishii*, only the southernmost population (*A. kishii*) exhibits reduced elytral grooves (Bergsten & Miller 2007). *Dytiscus sharpi* Wehncke, 1875 is divided into two subspecies: the nominate subspecies and *D. s. validus* Régimbart, 1899. *Dytiscus s. validus*, which possesses grooves on the female elytra, is distributed in higher-latitude regions, whereas the nominate subspecies, distributed in lower-latitude regions, lacks or has incomplete grooves on the female elytra (Mori & Kitayama 2002; Nakajima *et al*. 2020). Thus, it is noteworthy that populations distributed at the southernmost limits across multiple taxa tend to show a reduction of elytral striae and grooves. Modifications of the female elytra in Dytiscidae have been discussed in the context of sexual conflict (e.g., Bergsten & Miller 2007; Karlsson Green *et al*. 2013). Such modifications are typically observed only in females; therefore, it is remarkable that *A. zimmermanni* exhibits these traits in both sexes. *Austrelatus zimmermanni* thus represents an intriguing model for studying evolutionary processes and sexual conflict in Dytiscidae.

Acknowledgements

We express our sincere gratitude to Hiroyuki Yoshitomi (EUMJ), Shunpei Fujie (OMNH), and Atsushi Aimoto (Yamaguchi Prefecture) for the loan of supplying study material, Kei Hirasawa (Aquamarine Inawashiro Kingfishers Aquarium) for providing his collection material, Jun Nakajima (Fukuoka Institute of Health and Environmental Sciences), Shin-ya Ohba (Biological Laboratory, Faculty of Education, Nagasaki University) and Shigeyuki Yoshii (Fukushima Prefecture) for providing the information on *Austrelatus zimmermanni*, Tomo Hamano (The Graduate School of Human Science and Environment, University of Hyogo), Kei Hirasawa, Takayuki Ikegami (Graduate School of Science, Hokkaido University) for accompanying the field survey, Toshima Village and Kumejima-chô for providing the permission of insect collection, Jirí Hájek (NMPC) for his useful comments and loan of the Chinese material, Nobuyuki Narukawa (Mie Prefecture) for providing the documentation. We also thank Adrián Villastrigo (SNSB-Zoologische Staatssammlung München) for his advice regarding the molecular phylogenetic analysis, Norio Hirai (Graduate School of Agriculture, Osaka Metropolitan University) for partial financial support and for his valuable advice on this research, Hirokazu Fukutomi (IIM) for his support with microscopic observations, Hiroyuki Yoshitomi for his consent to deposit the specimen in the Museum. This study was partly supported by the Hoshizaki Green Foundation for KW, the Pro Natura Fund (35th Term, 2024) for MK, and the Austrian Science Fund (P 31347-B25) for HS.

References

Aimoto A. 2018. [A new record of *Copelatus zimmermanni* Gschwendtner, 1934 from Yamaguchi Prefecture]. *Sayabane, New Series* (29): 27−28. [In Japanese.]

Aoyagi M. 2022. Family Dytiscidae. *In*: Matsumura M., Kusui Y., Kohama T., Sasaki T., Aoyagi M. & Yoshitake H. (Eds) *Beetles of Okinawa*: 117–121. Okinawa Jiji Publishing Co., Naha. [In Japanese.]

Bergsten J. & Miller K.B. 2007. Phylogeny of diving beetles reveals a coevolutionary arms race between the sexes. *PloS ONE* 2 (6): e522. https://doi.org/10.1371/journal.pone.0000522

Bolger A.M., Lohse M. & Usadel B. 2014. Trimmomatic: a flexible trimmer for Illumina sequence data. *Bioinformatics* 30 (15): 2114–2120. https://doi.org/10.1093/bioinformatics/btu170

Bryant D. & Moulton V. 2004. Neighbor-net: an agglomerative method for the construction of phylogenetic networks. *Molecular Biology and Evolution* 21 (2): 255–265. https://doi.org/10.1093/molbev/msh018

Cho Y.B. & Kim D.S. 1998. Insect fauna of some wetlands in Cheju Island, Korea. *Bulletin of the KACN* 17: 57–74. [In Korean.]

Chung H.Y., Yeom C.M., Kim J.H., Park S., Lee Y.W., Pyo G. & Kim S.H. 2020. Species diversity and community characteristics of benthic macroinvertebrates from irrigation ponds in the western CCZ area, Korea. *Korean Journal of Ecology and Environment* 53: 173–184. https://doi.org/10.11614/KSL.2020.53.2.173

Colgan D.J., McLauchlan A., Wilson G.D.F., Livingston S.P., Edgecombe G.D., Macaranas J., Cassis G. & Gray M.R. 1998. Histone H3 and U2 snRNA DNA sequences and arthropod molecular evolution. *Australian Journal of Zoology* 46 (5): 419–437. https://doi.org/10.1071/ZO98048

ESK (The Entomological Society of Korea) & KSAE (Korean Society of Applied Entomology) 1994. *Check List of Insects from Korea*. Kon-Kuk University Press, Seoul.

Folmer O., Black M., Hoeh W., Lutz R. & Vrijenhoek R. 1994. DNA primers for amplification of mitochondrial cytochrome *c* oxidase subunit I from diverse metazoan invertebrates. *Molecular Marine Biology and Biotechnology* 3 (5): 294–299.

Fukagawa G. 2015. Record of water beetles (Noteridae, Dytiscidae, Gyrinidae, Hydrochidae, Hydraenidae and Hydrophilidae), in main land of Nagasaki Prefecture, Japan. *Transactions of the Nagasaki Biological Society* 76: 24–44. [In Japanese.]

Fukagawa G., Imasaka S., Yamamoto N., Noda M., Abiru N., Matsuo T. & Tanaka K. 2016. A fauna of the beetles (Coleoptera) in Nishisonogi peninsula, Nagasaki Pref., Japan. *Koganemushi* 81: 1–152. [In Japanese.]

Guéorguiev V.B. 1968. Essai de classification des coléoptères Dytiscidae. I. Tribus Copelatini (Colymbetinae). *Izvestija na Zoologitjeskija Instituts Musei Sofia* 28: 5–45.

Guéorguiev V.B. 1970. Dytiscidae (Coleoptera) nouveaux ou peu connus de l'Asie. *Izvestija na Zoologitjeskija Instituts Musei Sofia* 32: 253–260.

Hájek J. & Shaverdo H. 2024. Two new species of *Austrelatus* diving beetles from continental Southeast Asia, linking the distribution area of the genus (Coleoptera: Dytiscidae: Copelatinae). *Acta Entomologica Musei Nationalis Pragae* 64: 243–247. https://doi.org/10.37520/aemnp.2024.016

Hájek J., Shaverdo H., Hendrich L. & Balke M. 2021. A review of *Copelatus* diving beetles from the Solomon Islands, reporting the discovery of six new species (Coleoptera, Dytiscidae, Copelatinae). *ZooKeys* 1023: 81–118. https://doi.org/10.3897/zookeys.1023.61478

Hájek J., Alarie Y., Benetti C.J., Hamada N., Springer M., Hendrich L., Villastrigo A., Torres R.O., Basantes M.S. & Balke M. 2024. Underestimated diversity and range size of diving beetles in tank bromeliads — Coleoptera of 'hygrofloric' lifestyle (Dytiscidae). *Zoological Journal of the Linnean Society* 200: 720–735. https://doi.org/10.1093/zoolinnean/zlad093

Han M.S., Kim M.H., Bang H.S., Na Y.E., Lee D.B. & Kang K.K. 2011. Geographical distribution of diving beetles (Dytiscidae) in Korean paddy ecosystem. *Korean Journal of Environmental Agriculture* 30: 209−215. https://doi.org/10.5338/KJEA.2011.30.2.209

Hirano T., Kameda Y. & Chiba S. 2014. Phylogeny of the land snails *Bradybaena* and *Phaeohelix* (Pulmonata: Bradybaenidae) in Japan. *Journal of Molluscan Studies* 80 (2): 177−183. https://doi.org/10.1093/mollus/eyu004

Hosoya T. & Tanahashi M. 2017. New record of dytiscid beetle (Coleoptera, Dytiscidae) from Kuchinoshima Island in the Tokara Islands, the Ryukyu Archipelago, Japan. *Elytra, New Series* 7 (1): 15–16.

Hosoya T., Kiyoshi T. & Kawashimo Y. 2009. Records on aquatic Coleoptera in Takara Island, Tokara Islands, Kagoshima Prefecture, Japan. *Coleopterists' News* 165: 5–9. [In Japanese.]

Huson D.H. & Bryant D. 2024. The SplitsTree App: interactive analysis and visualization using phylogenetic trees and networks. *Nature Methods* 21 (10): 1773−1774. https://doi.org/10.1038/s41592-024-02406-3

Imasaka S., Hosoya T., Kokubu K., Ito R. & Arima K. 2021. [Collecting travelogue in Koshiki-shima Island, part 3 (July 2020)]. *Korasana* 96: 67–97. [In Japanese.]

Iwasaki I. & Kinoda T. 1995. New records of aquatic insects from Higashi-morokata district, Miyazaki Prefecture (Hemiptera & Coleoptera). *In*: Hirashima Y. (ed.) *Contribution to the Fauna and Flora of Miyazaki Higashimorokata District: New Records and Observations of Noteworthy Insects, Spiders and Plants Based on Systematic and Biologic Studies*: 101–111. Miyazaki Municipal University, Miyazaki, Japan.

Jiang Z.Y., Zhao S., Yang Z.Y., Jia F.L. & Hájek J. 2022. A review of *Copelatus* Erichson, 1832 of Mainland China, with description of ten new species from the *japonicus* complex (Coleoptera: Dytiscidae: Copelatinae). *Zootaxa* 5124 (3): 251–295. https://doi.org/10.11646/zootaxa.5124.3.1

Jiang Z.Y., Hájek J., Zheng Y.L., Jia F.L. & Wang B.X. 2025. Two new species of Oriental *Copelatus* Erichson, 1832, with additional records of the genus from China (Coleoptera: Dytiscidae: Copelatinae). *Zootaxa* 5632 (1): 42–50. https://doi.org/10.11646/zootaxa.5632.1.2

Jiang Z.Y., Zheng Y.L., Deng Z., Jia F.L. & Wang B.X. 2026. Two new species of *Copelatus* Erichson, 1832 from urban low mountains of eastern China, with new province records of the other Copelatinae in China (Coleoptera: Dytiscidae). *European Journal of Taxonomy* 1052: 105–124. https://doi.org/10.5852/ejt.2026.1052.3271

Kaito T. & Toda M. 2016. The biogeographical history of Asian keelback snakes of the genus *Hebius* (Squamata: Colubridae: Natricinae) in the Ryukyu Archipelago, Japan. *Biological Journal of the Linnean Society* 118 (2): 187–199. https://doi.org/10.1111/bij.12726

Kalyaanamoorthy S., Minh B.Q., Wong T.K., Von Haeseler A. & Jermiin L.S. 2017. ModelFinder: fast model selection for accurate phylogenetic estimates. *Nature Methods* 14 (6): 587–589. https://doi.org/10.1038/nmeth.4285

Kamite Y. 2003. [New records of dytiscid species from Minamidaitô-jima Island]. *Coleopterists' News* 143: 12. [In Japanese.]

Kamite Y., Aoyagi M. & Kamite N. 2019. Records on aquatic Coleoptera of Aka-jima and Geruma-jima, Okinawa Prefecture, Japan. *Sayabane, New Series* 36: 21–26. [In Japanese.]

Karlsson Green K., Kovalev A., Svensson E.I. & Gorb S.N. 2013. Male clasping ability, female polymorphism and sexual conflict: fine-scale elytral morphology as a sexually antagonistic adaptation in female diving beetles. *Journal of the Royal Society Interface* 10: e20130409. https://doi.org/10.1098/rsif.2013.0409

Kato M. & Watanabe K. 2025a. Records of eight aquatic insect species collected from Zamami–jima Island, the Ryukyus, Japan, including six new records (Hemiptera and Coleoptera). *Fauna Ryukyuana* 74: 1–6. [In Japanese.]

Kato M. & Watanabe K. 2025b. New distributional records of aquatic Coleoptera (Noteridae, Dytiscidae, Hydrophilidae) from Amami-Ôshima and Kakeroma-jima Islands, Kagoshima Prefecture, Japan. *Elytra, New Series* 15: 153–157.

Lee D.H. & Ahn K.J. 2018. *Insect Fauna of Korea, Volume 12, Number 22, Aquatic Coleoptera I, Arthropoda: Insecta: Coleoptera: Dytiscidae.* National Institute of Biological Resources, Incheon.

Lee S.H. 1991. A systematic study and distribution of Korean Dytiscidae. *Science Fair* 1991: 16–20. [In Korean].

Leigh J.W. & Bryant D. 2015. POPART: full-feature software for haplotype network construction. *Methods in Ecology & Evolution* 6 (9): 1110–1116. https://doi.org/10.1111/2041-210X.12410

Li Y.L. & Liu J.X. 2018. StructureSelector: a web-based software to select and visualize the optimal number of clusters using multiple methods. *Molecular Ecology Resources* 18 (1): 176–177. https://doi.org/10.1111/1755-0998.12719

Matsui E. 1987. [A new record of *Copelatus zimmermanni* Gschwendtner, 1934 from Kyushu, Japan]. *Gekkan-Mushi* (202): 5–6. [In Japanese.]

Matsui E. 1988. [Aquatic insect collection record in 1987 (Tanega-shima Island)]. *Satsuma* 37 (99): 1–10. [In Japanese.]

Matsui E. 1989. [A new record of *Copelatus zimmermanni* Gschwendtner, 1934 from Kume-jima Island, Okinawa Prefecture, Japan]. *Gekkan-Mushi* (226): 20. [In Japanese.]

Matsui E., Takai Y. & Tanabe T. 1988. Aquatic Coleoptera in Kagoshima Prefecture. *Satsuma* 37 (100): 61–115. [In Japanese.]

Matsui M. & Tominaga A. 2020. Distinct species status of a *Microhyla* from the Yaeyama Group of the Southern Ryukyus, Japan (Amphibia, Anura, Microhylidae). *Current Herpetology* 39 (2): 120–136. https://doi.org/10.5358/hsj.39.120

Miller K.B. & Nilsson A.N. 2003. Homology and terminology: Communicating information about rotated structures in water beetles. *Latissimus* 17: 1–4.

Mitamura T., Hirasawa K. & Yoshii S. 2017. *The Handbook of Japanese Aquatic Insect, Volume 1: Coleoptera*. Bun-ichi Sogo Shuppan, Tokyo. [In Japanese.]

Miyake T. 2021. [A new record of *Copelatus zimmermanni* Gschwendtner, 1934 from Ôita Prefecture, Japan]. *Nihônomushi* 59: 100. [In Japanese.]

Mori M. & Kitayama A. 2002. *Dytiscoidea of Japan*. Bun-ichi Sogo Shuppan, Tokyo. [In Japanese.]

Morii T. 2018. [A new record of *Copelatus zimmermanni* Gschwendtner, 1934 from Amami-ôshima Island, Japan]. *Sayabane, New Series* 29: 5. [In Japanese.]

Nakajima J. & Inoue D. 2004. [Records of *Copelatus zimmermanni* Gschwendtner, 1934 from Fukuoka Prefecture]. *Coleopterists' News* 148: 14. [In Japanese.]

Nakajima J., Hayashi M., Ishida K., Kitano T. & Yoshitomi H. 2020. *Aquatic Coleoptera and Hemiptera of Japan*. Bun-ichi Sogo Shuppan, Tokyo. [In Japanese.]

Nakamine A. & Nakamine K. 2021. Records of aquatic insects collected on Tanegashima Island in 2020. *Bulletin of the Kagoshima Prefectural Museum* 40: 1–8. [In Japanese.]

Nakane T. 1963. New or little-known Coleoptera from Japan and its adjacent regions XVIII. *Fragmenta Coleopterologica* 6: 23–26.

Narukawa N., Ichihashi H., Nakanishi M. & Kawakita H. 2006. [*Insect Fauna of the Kumanonada Costal Laurel Forest*.] Mie Konchû Danwakai, Matsusaka. [In Japanese.]

Nilsson A.N. & Hájek J. 2026. *A World Catalogue of the Family Dytiscidae, or the Diving Beetles (Coleoptera, Adephaga) Version 1.I.2026*. Available from http://www.waterbeetles.eu [accessed 12 May 2026].

Nomura S., Mizokami S. & Ôtsuka K. 1996. [Aquatic Coleoptera of Saga Prefecture, Japan]: 249–262. Sagaken no Seibutsu.

Ôtsuka I. 1991. [A new record of *Copelatus zimmermanni* Gschwendtner, 1934 from the Amakusa Islands, Japan]. *Gekkan-Mushi* 240: 39. [In Japanese.]

Papadopoulou A., Anastasiou I. & Vogler A.P. 2010. Revisiting the insect mitochondrial molecular clock: the mid-Aegean trench calibration. *Molecular Biology and Evolution* 27 (7): 1659–1672. https://doi.org/10.1093/molbev/msq051

Park H.C., Lee Y.B. & Lee H.A. 2008. Taxonomic review of the genus *Copelatus* Erichson (Coleoptera: Dytiscidae) in Korea. *Entomological Research* 38 (1): 73–76. https://doi.org/10.1111/j.1748-5967.2008.00134.x

Pritchard J.K., Wen X. & Falush D. 2009. *Documentation for Structure Software: Version 2.3*. University of Chicago, Chicago.

QGIS Development Team 2024. QGIS Geographic Information System. Open Source Geospatial Foundation Project. Available from https://qgis.org/ [accessed 22 Dec. 2025].

R Core Team 2020. R: A language and environment for statistical computing. R Foundation for Statistical Computing, Vienna, Austria. Available from https://www.r-project.org/ [accessed 22 Dec. 2025].

Rambaut A. 2009. FigTree version 1.4.4. Available from https://tree.bio.ed.ac.uk/software/figtree/ [accessed 4 Mar. 2026].

Ranarilalatiana T. & Bergsten J. 2019. Discovery of a specialist Copelatinae fauna on Madagascar: highly ephemeral tropical forest floor depressions as an overlooked habitat for diving beetles (Coleoptera, Dytiscidae). *ZooKeys* 871: 89–118. https://doi.org/10.3897/zookeys.871.36337

Ranarilalatiana T., Harivelo L., Ravaomanarivo R. & Bergsten J. 2019. Taxonomic revision of the *Copelatus* of Madagascar (Coleoptera, Dytiscidae, Copelatinae): the non-*erichsonii* group species. *ZooKeys* 871: 89–118. https://doi.org/10.3897/zookeys.869.33997

Régimbart M. 1899. *Révision des Dytiscidae de la Région Indo-Sino-Malaise. Annales de la Société entomologique de France* 68: 186–367. Available from https://www.biodiversitylibrary.org/page/8431385 [accessed 22 Dec. 2025].

Rochette N.C., Rivera-Colón A.G. & Catchen J.M. 2019. Stacks 2: analytical methods for paired-end sequencing improve RADseq-based population genomics. *Molecular Ecology* 28 (21): 4737–4754. https://doi.org/10.1111/mec.15253

Sakurai S. 1992. [Records of three *Copelatus* species from Chôkaisan, Honshu, Japan]. *Gekkan-Mushi* 262: 20–21. [In Japanese.]

Sato F. 2004. [Records of *Copelatus zimmermanni* Gschwendtner, 1934 from Oga Peninsula, Akita Prefecture]. *Gekkan-Mushi* 406: 8. [In Japanese.]

Satô M. 1983. Distribution of the genus *Copelatus* in Japan (Coleoptera: Dytiscidae). *In*: Satô M. (ed.) *Special Issue Concerning the Aquatic Coleoptera Presented at the Workshop of the XVI International Congress of Entomology in Kyoto, Japan in 1980*: 35–41. Nagoya.

Satô M. 1984. Taxonomic notes on the aquatic Coleoptera of Japan, II. *Coleopterists' News* 66: 1–4. [In Japanese.]

Satô M. 1985. The genus *Copelatus* of Japan (Coleoptera: Dytiscidae). *Transactions of the Shikoku Entomological Society* 17: 57–67.

Satô M. 1998. Aquatic Coleoptera of the Ryukyu archipelago, III. *Coleopterists' News* 121: 7–13. [In Japanese.]

Shaverdo H. & Balke M. 2022. A species-group key and notes on phylogeny and character evolution in New Guinean *Exocelina* Broun, 1886 diving beetles (Coleoptera, Dytiscidae, Copelatinae). *ZooKeys* 1131: 31–58. https://doi.org/10.3897/zookeys.1131.94205

Shaverdo H., Surbakti S., Hendrich L. & Balke M. 2012. Introduction of the *Exocelina ekari*-group with descriptions of 22 new species from New Guinea (Coleoptera, Dytiscidae, Copelatinae). *ZooKeys* 250: 1–76. https://doi.org/10.3897/zookeys.250.3715

Shaverdo H., Hájek J., Hendrich L., Surbakti S., Panjaitan R. & Balke M. 2023. *Austrelatus* gen. nov., a new genus of Australasian diving beetles (Coleoptera, Dytiscidae, Copelatinae), with the discovery of 31 new species from New Guinea. *ZooKeys* 1170: 1–164. https://doi.org/10.3897/zookeys.1170.103834

Shaverdo H., Hendrich L., Surbakti S., Panjaitan R. & Balke M. 2024. Revision of the *Austrelatus papuensis* group with descriptions of 42 new species from New Guinea (Coleoptera, Dytiscidae, Copelatinae). *ZooKeys* 1201: 1–165. https://doi.org/10.3897/zookeys.1201.116131

Shaverdo H., Wewalka G., Hendrich L. & Balke M. 2026 (in preparation). Revision of the *Austrelatus* species of Fiji (Coleoptera, Dytiscidae, Copelatinae), with descriptions of 29 new species and notes on Copelatinae species of the Pacific Islands.

Sheth S.D., Ghate H.V. & Hajek J. 2018. *Copelatus* Erichson, 1832 from Maharashtra, India, with description of three new species and notes on other taxa of the genus (Coleoptera: Dytiscidae: Copelatinae). *Zootaxa* 4459 (2): 235–260. https://doi.org/10.11646/zootaxa.4459.2.2

Suyama Y. & Matsuki Y. 2015. MIG-seq: an effective PCR-based method for genome-wide single-nucleotide polymorphism genotyping using the next-generation sequencing platform. *Scientific Reports* 5 (1): 16963. https://doi.org/10.1038/srep16963

Suyama Y., Hirota S.K., Matsuo A., Tsunamoto Y., Mitsuyuki C., Shimura A. & Okano K. 2022. Complementary combination of multiplex high-throughput DNA sequencing for molecular phylogeny. *Ecological Research* 37 (1): 171–181. https://doi.org/10.1111/1440-1703.12270

Tahira Y. & Kitano T. 2000. [Records of *Copelatus zimmermanni* Gschwendtner, 1934 from Nirayama-cho, Shizuoka Prefecture]. *Gekkan-Mushi* 357: 44−45. [In Japanese.]

Takahashi M. 1994. [Records of *Copelatus zimmermanni* Gschwendtner, 1934]. *Coleopterists' News* 105: 5–6. [In Japanese.]

Tamu N. & Tsukamoto K. 1955. [On the Coleoptera in Kammuri Island (Kyoto, Japan) I (Studies on the insects in small islands, I)]. *Akitu* 4: 69–76. [In Japanese.]

Tamura K., Stecher G. & Kumar S. 2021. MEGA11: molecular evolutionary genetics analysis version 11. *Molecular Biology and Evolution* 38 (7): 3022–3027. https://doi.org/10.1093/molbev/msab120

Thompson J.D., Higgins D.G. & Gibson T.J. 1994. CLUSTAL W: improving the sensitivity of progressive multiple sequence alignment through sequence weighting, position-specific gap penalties and weight matrix choice. *Nucleic Acids Research* 22 (22): 4673–4680. https://doi.org/10.1093/nar/22.22.4673

Watanabe K. 2022. Biological notes on immature stages of *Platambus ussuriensis* (Nilsson, 1997) and *Copelatus nakamurai* Guéorguiev, 1970 (Coleoptera: Dytiscidae). *The Coleopterists Bulletin* 76 (2): 233–236. https://doi.org/10.1649/0010-065X-76.2.233

Watanabe K. 2025. Review of Dytiscidae (Coleoptera) eggs: focus on Japanese species. *Journal of Insect Conservation* 29: 1. https://doi.org/10.1007/s10841-024-00636-6

Watanabe K. & Hayashi M. 2019. Reproductive ecology and immature stages of *Copelatus masculinus* Régimbart, 1899 (Coleoptera, Dytiscidae). *Elytra, New Series* 9 (2): 269–278.

Watanabe K. & Ohba S. 2022. Life history of *Copelatus zimmermanni* Gschwendtner, 1934 (Coleoptera: Dytiscidae) and the ecological significance of the larval period of three *Copelatus* species. *Entomological Science* 25 (2): e12505. https://doi.org/10.1111/ens.12505

Watanabe K. & Yoshitomi H. 2022 [2023]. Family Dytiscidae. *In*: the Editorial Committee of Catalogue of the Insects of Japan (ed.) *Catalogue of the Insects of Japan, 6. Coleoptera, Part 1*: 8–27. Touka Shobo, Fukuoka. [In Japanese.]

Watanabe K., Hayashi M. & Kato M. 2017. Immature stages and reproductive ecology of *Copelatus parallelus* Zimmermann, 1920 (Coleoptera, Dytiscidae). *Elytra, New Series* 7 (2): 361–374.

Watanabe K., Hayashi M. & Nagashima S. 2024. Life history of *Copelatus kammuriensis* Tamu and Tsukamoto, 1955 (Coleoptera: Dytiscidae: Copelatinae) and biological implications. *Aquatic Insects* 45 (2): 285–297. https://doi.org/10.1080/01650424.2023.2253250

Watanabe N., Arai K., Otsubo M., Toda M., Tominaga A., Chiyonobu S., Sato T., Ikeda T., Takahashi A., Ota H. & Iryu Y. 2023. Geological history of the land area between Okinawa Jima and Miyako Jima of the Ryukyu Islands, Japan, and its phylogeographical significance for the terrestrial organisms of these and adjacent islands. *Progress in Earth and Planetary Science* 10 (1): 40. https://doi.org/10.1186/s40645-023-00567-x

Wong T.K.F., Ly-Trong N., Ren H., Demotte P., Baños H., Roger A.J., Susko E., Bielow C., de Maio N., Goldman N., Hahn M.W., dos Reis M., Vinh L.S., Huttley G., Lanfear R. & Minh B.Q. 2026. IQ-TREE 3: phylogenomic inference software using complex evolutionary models. *Molecular Biology and Evolution* 43 (5): msag117. https://doi.org/10.1093/molbev/msag117

Zimmermann A. 1920. Bemerkenswerte Neuerwerbungen des Zoologischen Museums in Hamburg. Haliplidae, Dytiscidae et Gyrinidae. *Entomologische Blätter* 16: 224–234. Available from https://www.biodiversitylibrary.org/page/34024158 [accessed 22 Dec. 2025].

Zimmermann A. 1934. Monographie der paläarktischen Dytisciden. V. Colymbetinae (1. Teil). *Koleopterologische Rundschau* 20: 138–214.

Printed versions of all papers are deposited in the libraries of two of the institutes that are members of the *EJT* consortium: Muséum national d'Histoire naturelle, Paris, France and Royal Museum for Central Africa, Tervuren, Belgium. The other members of the consortium are: Royal Belgian Institute of Natural Sciences, Brussels, Belgium; Meise Botanic Garden, Meise, Belgium; Natural History Museum of Denmark, Copenhagen, Denmark; Naturalis Biodiversity Center, Leiden, the Netherlands; Museo Nacional de Ciencias Naturales-CSIC, Madrid, Spain; Leibniz Institute for the Analysis of Biodiversity Change, Bonn – Hamburg, Germany; National Museum of the Czech Republic, Prague, Czech Republic; The Steinhardt Museum of Natural History, Tel Aviv, Israël.

Supplementary file

Supp. file 1. Maximum likelihood phylogenetic tree based on the dataset 2 (599 bp of the mitochondrial *COI* gene). The area enclosed by the blue rectangle represents specimens of *Austrelatus zimmermanni* (Gschwendtner, 1934) collected in Japan. The values near the nodes of the phylogenetic tree are the ultrafast bootstrap values, and they are shown when the values are 70 or higher.
https://doi.org/10.5852/ejt.2026.1098.3329.14615